NASA Technical Memorandum 83301

BLOCKAGE AND FLOW STUDIES OF A GENERALIZED TEST APPARATUS INCLUDING VARIOUS WING CONFIGURATIONS IN THE LANGLEY 7-INCH MACH 7 PILOT TUNNEL

CINDY W. ALBERTSON

MARCH 1982

NASA

National Aeronautics and
Space Administration

Langley Research Center
Hampton, Virginia 23665

SUMMARY .

A 1/12th scale model of the Curved Surface Test Apparatus (CSTA), which will be used to study aerothermal loads and evaluate Thermal Protection Systems (TPS) on a fuselage-type configuration in the Langley 8-Foot High Temperature Structures Tunnel (8' HTST), was tested in the Langley 7-Inch Mach 7 Pilot Tunnel. The purpose of the pilot tunnel tests was to study the overall flow characteristics and define an envelope for testing the CSTA in the 8' HTST. This envelope is defined by the model angle of attack and tunnel operating pressures at which the flow field around the model remains realistic. Tests were then conducted using the scaled CSTA model with various wing configurations to select a wing geometry with the most favorable characteristics for conducting TPS evaluations for curved and intersecting surfaces. The test envelope of the selected wing configuration, which is beveled 30° on the wing leading edge, was also obtained.

Results indicate that the CSTA can be tested with no shock interference at angles of attack up to 15.5 degrees for combustor pressures above 580 psia. For the same pressure range, the wing configuration can be tested at angles of attack up to 10.5 degrees. The base pressure for the CSTA model and wing configuration was at the expected low level for most test conditions. However, a high base pressure was obtained at certain test conditions in which ambient temperature air was used as the test medium. Improved performance was demonstrated for high temperature conditions, using combustion products as the test medium, but the possibility of a high base pressure should be evaluated during the initial flow studies in the 8' HTST. The tunnel operational performance for both the CSTA model and wing configuration was representative of the performance for a small to medium blockage model for the range of angles of attack tested. Results generally indicate that the CSTA and wing

configuration will provide a useful test bed for aerothermal loads and thermal structural concept evaluation over a broad range of flow conditions in the 8' HTST.

INTRODUCTION

A large generalized test apparatus representing the forward portion of a fuselage is being developed for aerothermal loads and Thermal Protection System (TPS) concept research in the Langley 8-Foot High-Temperature Structures Tunnel (8' HTST). This apparatus, which is refered to as the Curved Surface Test Apparatus (CSTA), will be used to determine the detailed aerothermal loads associated with fuselage-type bodies. These loads will be defined in terms of pressure and heating-rate distributions over a range of hypersonic flight conditions. Particular emphasis will be placed on defining loads in the windward and leeward chine regions. The apparatus will also function as a test bed for flat and curved Thermal Protection System (TPS) evaluations. Wings will be added to the apparatus to evaluate intersecting TPS concepts at the wing-body juncture.

The size and shape of the test apparatus for open jet wind tunnels such as the 8' HTST can be critical to test results since the flow blockage caused by the apparatus can prevent the development of hypersonic flow in the test region. For less severe blockage situations in which the flow in the test region is hypersonic, excessive test chamber pressure may exist and result in shock interference with the local flow around the model. Therefore, a flow and blockage study was conducted in the Langley 7-Inch Mach 7 Pilot Tunnel, which is a geometrically scaled version of the 8' HTST, using scaled models to determine a range of conditions at which the CSTA with and without wings can be tested. A total of seven wing configurations were tested to select a wing geometry with the most favorable flow and tunnel operational characteristics.

2

Tests were conducted for various model angles of attack using air and combustion products at total temperatures of 500 and 3060 R, respectively, for total pressures ranging from 580 to 2180 psia. These temperature conditions correspond to free stream Mach numbers of 5.3 and 6.8, respectively. Tunnel flow effects were observed using schlieren photography and oil-flow techniques. The results of this study, presented within this report, indicate the expected CSTA performance for the full scale tests in the 8' HTST. It also shows some of the adverse effects on the model flow field which can occur in high-speed wind tunnels for excessive flow blockage conditions.

SYMBOLS

P_b	model base pressure, psia
P_c	test chamber pressure, psia
P_e	nozzle exit pressure, psia
P_{tc}	combustor total pressure, psia
P_{tj}	ejector total pressure, psia
T_{tc}	combustor total temperature, R
α	angle of attack, degrees (referenced from model center line as illustrated in figure 2)

APPARATUS AND TESTS

Models

The blockage model of the Curved Surface Test Apparatus (CSTA) is approximately a 0.083 (or 1/12th) scale version of the 8' HTST apparatus.

3

However, since the geometric scale factor between the pilot tunnel and the 8' HTST is 0.078, the pilot tunnel model tests will yield a conservative estimate of the 8' HTST performance. Photographs of the CSTA model are presented in figure 1, and drawings of the model including pertinent dimensions are given in figure 2. The model is 9.70 in. long and 3.02 by 2.00 in. at the base. The nose of the model is spherically shaped with a 0.25 in. radius. The model has wedge half angles of 7.59° and 4.50° as shown by the top and side views in figure 2. The chine radii increase linearly along the length of the model to a maximum of 1.00 in. and 0.33 in. on the top and bottom, respectively.

A total of seven wing configurations, as shown in figure 3, were tested to determine a configuration with the most favorable flow characteristics. Configurations I, II, and III were tested to study the effect of wing planform area variation on flow blockage. The basic wing shape was selected to represent that of a Shuttle Orbiter and wing thickness was determined from TPS requirements. Configurations II, IV, V, VI and VII were tested to study the effect of leading edge variations on flow blockage. All seven are swept back 45 degrees and have a delta wing planform with truncated wing tips. The first six have a 3.5° dihedral angle while the seventh wing has zero dihedral. More specific details of each wing configuration follow.

Configuration I. - This is the largest wing configuration (fig. 3a) tested. The tip chord length and span are 2.25 and 7.00 in., respectively, resulting in a 0.32 ratio between the two. The leading edge is cylindrically shaped and fairs into a 0.66 in. wing thickness.

Configuration II. - This configuration (fig. 3b) is the same as configuration I except for a reduction in wing planform area. The tip chord length is reduced in proportion to the span to maintain approximately a 0.32 ratio. The resulting lengths are 2.00 and 6.00 in., respectively.

4

Configuration III. - This configuration (fig. 3c) is the same as configurations I and II but has a further reduction in planform area, again maintaining approximately a 0.32 ratio between the wing tip chord length and span. The lengths are 1.55 and 5.00 in., respectively.

Configuration IV. - This configuration (fig. 3d) has the same planform area as configuration II but has half the wing thickness and hence, half the leading edge radius of configurations I, II, and III.

Configuration V. - This configuration (fig. 3e) has the same planform area excluding leading edge and the same wing thickness as configuration II but has a wing tip chord length equal to that of configuration I. The leading edge cross section geometry is an approximate ellipse represented by two connecting radii of 0.17 and 1.75 in. as indicated in the figure.

Configuration VI. - This configuration (fig. 3f) is the same as configuration V but has a symmetric bevel leading edge cross-section geometry. The half angle of the bevel is 21°.

Configuration VII. - This configuration (figs. 3g and 4) has the same planform as configuration V and VI but has a 30° bevel leading edge cross-section geometry and a reduced wing thickness of 0.50 in. The leading edge is slightly blunted and has a 0.015 in. radius. A fairing was added at the wing leading edge and body junction to improve local flow conditions as shown in figure 4.

Facility

Each configuration was tested in the Langley 7-Inch Mach 7 Pilot Tunnel (7" M7PT), illustrated in figure 5. This facility is a hypersonic blowdown wind tunnel capable of simulating the aerothermal flight environment at a nominal Mach number of 7 in the altitude range between 82,000 and 131,000 ft.

To achieve these conditions, air and methane are burned under high pressure in the combustion chamber. The combustion products, which serve as the test medium, are then expanded through a conical-contoured nozzle to a nominal Mach number of 7 and flow through a free jet test chamber. The gases are compressed in a supersonic diffuser and then enter a mixing-tube where air from the ejector is introduced to aspirate the gases including the portion which tends to stagnate in the test chamber. This process facilitates tunnel starting and allows tunnel operation at lower total pressures. The resulting mixture then flows through a subsonic diffuser (not shown) to the atmosphere. Prior to tunnel starting, the sting mounted model is held out of the stream until test conditions are established. The model is then rapidly inserted into the stream by means of a hydraulically actuated mechanism which requires approximately one second to position the model. The tunnel operates within a combustor total temperature and pressure range of 2470 to 3600 R and 400 to 2500 psia, respectively. For special tunnel performance checks the tunnel can be operated within the same pressure range using ambient temperature air (500 R) as the test medium. This is often done for blockage studies because of the reduced time involved in preparing the tunnel for tests and because previous experience has shown good correlation between blockage results obtained using the two test media.

Tests

All models were inverted and pitched at a negative angle of attack for most tests to avoid tunnel unstart during model entry into the stream. Each model was initially tested in ambient temperature air (T_{tc} = 500 R), corresponding to a Mach number of 5.3, at p_{tc} = 1740 psia to establish the allowable range of angles of attack for each model and then to determine the most favorable wing geometry. The CSTA model and selected wing configuration

6

(configuration VII) were then tested at additional pressures and using the products of combustion as the test medium (T_{tc} = 3060 R), corresponding to a Mach number of 6.8, to establish the complete test envelope for the large scale tests. Oil flow visualization was used for these models at large angles of attack to obtain generalized flow patterns and as an additional check for adverse flow conditions.

The tunnel operational characteristics were determined for the CSTA and selected wing configuration (configuration VII) by first starting the tunnel with the air ejector operating at an excessive pressure and at a particular combustor total temperature and pressure. The model was brought into the stream after conditions were established and the ejector pressure was reduced until the flow became subsonic or until there was no flow through the ejector. This was done for combustor total pressures ranging from 580 to 2180 psia using air (T_{tc} = 500 R) and combustion products (T_{tc} = 3060 R).

The tunnel data consisting of temperatures and pressures and the model base pressure data were obtained by recording the output of platinum-platinum (13 percent rhodium) thermocouples and diaphragm type pressure transducers. The outputs were recorded with a Beckman 210 digital recording system sampling at a rate of 20 times per second and then reduced to give the proper temperatures and pressures. A single pass, Z-type schlieren system with a continuous light source was used to obtain photographs of the shock patterns around the model at a rate of 10 frames per second.

RESULTS AND DISCUSSION

CSTA Model

Shock interference. - Even though the flow may remain hypersonic once the model is in the stream, local flow conditions may exist which are not

representative of hypersonic flight conditions. An example of this is shock wave interference with the model flow field, as illustrated in figure 6. The presence of the model creates an energy loss in the flow and may cause a portion of the flow to be diverted outside the diffuser. The latter will be accompanied by a pressure rise in the test chamber if the ejector is unable to aspirate the diverted flow which stagnates in this region. When the test chamber pressure, p_c, is larger than the nozzle exit pressure, p_e, a compression shock cone forms at the nozzle exit at an angle Θ which is dependent upon the ratio p_c/p_e. This shock is more of a concern with long models since a pressure ratio slightly above 1.0 can produce a shock which will interfere with the model flow field.

The test chamber to nozzle exit pressure ratio as a function of angle of attack and combustor total pressure is shown in figure 7. The unticked data correspond to tests in which ambient temperature air (T_{tc} = 500 R) was used as the test medium. The ticked data was obtained using the products of combustion as the test medium (T_{tc} = 3060 R). Pressure ratios below 1.0 indicate that the flow is underexpanded at the nozzle exit and continues to expand in the test chamber region. Pressure ratios above 1.0 indicate that the flow is overexpanded and a compression shock cone is generated at the nozzle exit. As shown in figure 7, p_c/p_e generally increased with increasing α and with decreasing combustor pressure, suggesting possible shock interference at higher angles of attack. The figure also shows that the test medium (air or combustion products) had little effect. Schlieren photographs, shown in figure 8 for variations of α at p_{tc} = 1740 psia, were used to determine if the conical shock interfered with the flow field around the model. Shock interference did not occur for these test conditions for α ranging from -4.5 to 15.5° as expected since p_c/p_e ranged from 0.83 to 1.02.

8

However, for $\alpha = 20.5°$, where $p_c/p_e = 1.31$, shock interference did occur as shown by the schlieren photograph. This test condition was run using ambient temperature air only. The effect of combustor total pressures on the flow quality is illustrated by the schlieren photographs in figure 9 which are shown for various total pressures at $\alpha = -4.5$ and $15.5°$. For $\alpha = -4.5°$, where p_c/p_e was 1.1 for $p_{tc} = 580$ psia, shock interference is not indicated in the schlieren photograph. However, at $\alpha = 15.5°$ where p_c/p_e was 1.41 for $p_{tc} = 580$ psia, shock interference is indicated in the schlieren photograph. Hence values of p_c/p_e slightly greater than 1.0 are tolerable.

In both cases where shock interference occurred, the model was only tested using ambient temperature air. There is a possibility that interference will not occur using combustion products because the Mach number is higher hence the shock strength is lower. In addition, the pilot tunnel blockage results would tend to be conservative in predicting the blockage results of the CSTA in the 8' HTST, as discussed earlier. However, the possiblity of shock interference at these conditions should be evaulated during the initial flow studies with the CSTA in the 8' HTST. Generally, these tests indicate that the CSTA can be tested from $\alpha = -4.5$ to $15.5°$ for total pressures ranging from 1160 to 1740 psia, but trends in the data indicate that tests can be made at higher total pressures. Tests can also be made from $\alpha = -4.5$ to $5.5°$ for $p_{tc} = 580$ psia, as indicated by the data in figure 7.

Model base pressure. - Normally the base pressure of models tested in the 8' HTST is low relative to the free stream pressure and is of no concern during aerothermal tests. However under certain test conditions a high base pressure may occur which can adversely affect local flow conditions and possibly damage instrumentation inside the model by forcing in hot gases. A

9

possible source of the high base pressure is the interaction of the flow in the supersonic diffuser and test section as illustrated in figure 10. Possible flow conditions corresponding to a low and high base pressure are shown, however, the exact shock formation is unknown since the schlieren does not include the diffuser. The assumed shock pattern consists of a Mach disk created by the intersecting compression shocks formed at the entrance to the supersonic diffuser. The size of the Mach disk and the attendant subsonic flow region is dependent on the compression shock strength. When the wake converges ahead of the diffuser shock system, as shown in figure 10(a), a low pressure circulation region is formed at the base region of the model. If convergence does not occur, the higher pressure in the subsonic region behind the Mach disk in the diffuser may feed forward into the base region as illustrated in figure 10(b). Because of the inability to predict when this phenomena will occur, the base pressure should be checked over a range of conditions during blockage tests.

The CSTA model base pressure to nozzle exit pressure ratio, p_b/p_e, was plotted over a range of ejector pressures in figure 11 for α = -4.5, 5.5, and 15.5° and p_{t_c} = 580, 1160, and 1740 psia. The base pressure remained low and stable in all cases except for the high pressure runs conducted at α = 5.5° using air as the test medium. At p_{t_c} = 1160 psia, the base pressure was high throughout the range of ejector pressure settings. At p_{t_c} = 1740 psia, however, the base pressure was high only for ejector pressures below 305 psia. Since tests using combustion products were not conducted at these conditions, it is not certain whether this phenomena will occur in the 8' HTST. The possibility of a high base pressure at these conditions should be evaluated during the initial flow studies in the 8' HTST.

Oil flow pattern. - Oil flow patterns were obtained for the CSTA model to better understand the model flow field and to provide an additional check on

the possibility of shock interference. A typical oil flow pattern, shown in figure 12, was obtained in air at p_{tc} = 1740 psia and α = 15.5°, the highest angle the CSTA model can be tested. The flow appears to be attached on all surfaces except along the chines on the leeward surface.

Tunnel operational characteristics. - To minimize air consumption for the purpose of minimizing energy usage or maximizing run times, the 8' HTST is generally operated at approximately 50 psia above the minimum ejector pressure needed to maintain hypersonic flow. The pressure required is dependent upon the losses associated with the particular model as well as the combustor total pressure.

The minimum tunnel operating characteristics, in terms of combustor and ejector total pressures, are shown in figure 13 for the CSTA at α = -4.5, 5.5, and 15.5° for air and combustion products at T_{tc} = 500 and 3060 R, respectively. The faired curve represents the overall minimum tunnel operating boundary for the CSTA. Tunnel operation below the boundary results in subsonic flow in the test chamber while operation above the boundary results in hypersonic flow. This boundary is between the standard 7" M7PT minimum operating boundaries for a large model blockage and no model blockage, as shown in the figure and, hence, the CSTA is considered a small to medium blockage model.

Wing Configurations

The test chamber to nozzle exit pressure ratio and schlieren photographs were used to qualitatively evaluate the blockage effects of seven wing configurations. The pressure ratios are plotted for each configuration at various angles of attack as shown in figure 14. The results from tests in air (T_{tc} = 500 R) and combustion products (T_{tc} = 3060 R) were obtained at p_{tc} = 1740 psia and are denoted by unticked and ticked symbols, respectively. Typical schlieren photographs of each configuration are shown in figure 15.

Configurations I through III were used to study the effect of planform area on flow blockage. Configurations I and II could not be tested at any angle without shock interference while configuration III could only be tested at $\alpha = 0.5°$. Tests with these first three models revealed that flow disturbances generally decreased with decreasing planform area since frontal area was reduced.

Since higher angles of attack are required for TPS evaluations using the full scale CSTA in the 8' HTST, it was necessary to deviate from the initial objective of using a relatively thick wing with a blunt leading edge, characteristic of the first three configurations. Configuration IV was tested to study the effect of wing thickness on blockage even though the wing itself is thinner than TPS studies require. As expected, the reduced thickness allowed the model to be tested at a higher angle of attack ($\alpha = 5.5°$). This result also suggested that the leading edge geometry may have a significant effect on performance. Configurations V and VI were added to further study leading edge effects on blockage. The leading edges of both wings were streamlined to improve local flow conditions by decreasing total pressure losses across the bow shock, and their performance indicated smaller stream pressure losses than the initial set of cylindrical leading edges. Configuration VI produced a greater pressure loss than configuration V which was unexpected since the wing leading edge of this configuration was beveled so that the bow shock would remain attached. At low angles of attack this would reduce pressure losses and, hence, blockage effects. At higher angles however, the windward side of the bevel apparently caused a significant portion of the flow to be deflected away from the tunnel diffuser and into the test chamber. The pressure ratios (fig. 14) and schlieren photographs (fig. 15b), generally indicated the need for a thinner wing with a more streamlined

12

leading edge if a higher angle of attack was to be obtained. Therefore, wing configuration VII (fig. 4) was designed to be slightly thinner (thickness determined to accommodate required TPS thickness for a reduced angle of attack) with a leading edge which is beveled such that much of the flow is deflected to the leeward side of the model towards the diffuser. Test results (fig. 14) show that configuration VII has the most favorable performance of any of the configurations tested and hence has been selected for the 8' HTST apparatus. The normalized test chamber pressures were below 1.0 at α = -4.5, 0.5 and 5.5° and slightly above 1.0 ($p_c/p_e \approx 1.1$) at α = 10.5°.

Selected Wing Configuration

Shock interference. - The test chamber to nozzle exit pressure ratios were plotted against angle of attack in figure 16 at various tunnel operating conditions. The unticked data correspond to tests in which ambient temperature air (T_{tc} = 500 R) was used as the test medium while the ticked data was obtained from tests using the products of combustion at T_{tc} = 3060 R. Generally, the blockage increased with increasing α, suggesting possible shock interference at higher angles of attack. This trend is supported by the schlieren photographs in figure 17, which are shown for various angles of attack at a total pressure of 1740 psia and temperatures of 500 and 3060 R for air and combustion products, respectively. Shock interference did not occur at this total pressure for α ranging from -4.5 to 5.5° (where p_c/p_e ranged from 0.87 to 0.98) but was indicated in the schlieren photograph for α = 10.5° where p_c/p_e = 1.17. However, at the same angle of attack (α = 10.5°) for T_{tc} = 3060 R where p_c/p_e = 1.14, shock interference did not occur. This is attributed to the increased Mach number (5.3 to 6.8) resulting in a lower strength compression wave which does not interfere with the model flow field. Figure 16 also shows that p_c/p_e increased with decreasing p_{tc} indicating

13

possible shock interference at lower total pressures, particularly at high angles of attack. The schlieren photographs in figure 18 show shock interference at P_{tc} = 580 psia, α = -4.5° (p_c/p_e = 1.4) and for all conditions at α = 10.5° (p_c/p_e > 1.15) with air as the test medium (T_{tc} = 500 R). However for the two tests at T_{tc} = 3060 R for α = 10.5°, shock interference did not occur. Consequently, as discussed previously, shock interference may not occur during 8' HTST tests. These effects will be determined during the initial flow studies with the CSTA in the 8' HTST. Generally, the 7" M7PT tests indicate that the model can be tested from α = -4.5 to 10.5° for total pressures ranging from 1160 to 2180 psia. Trends in the data also indicate that tests can be made at higher total pressures. In addition, tests can be made from α -4.5 to 5.5° for p_{tc} = 580 psia.

Model base pressure. - The base pressure to nozzle exit pressure ratio, p_b/p_e, was plotted over a range of ejector pressures in figure 19 for α = -4.5° and 10.5° and p_{tc} = 580, 1160, 1740, and 2180 psia. At α = -4.5° the base pressure was high during tests conducted at p_{tc} = 1470 and 2180 psia using air (T_{tc} = 500 R). However, one test conducted at p_{tc} = 1740 psia and p_{tj} = 460 psia using combustion products (T_{tc} = 3060 R) resulted in a low base pressure. Tests at all other conditions also resulted in a low base pressure. Since a low base pressure was obtained during the test at α = -4.5° for p_{tc} = 1740 psia using combustion products, the flow conditions may be satisfactory for all 8' HTST tests conducted at the normally high temperature condition.

Oil flow pattern. - Characteristics similar to those obtained for the CSTA model appear in the oil flow patterns for configuration VII at α = 10.5° for p_{tc} = 1740 psia using air as shown in figure 20. The flow is apparently attached on all surfaces except the leeward chines. A flow disturbance is

14

indicated on the leeward wing leading edge surface and is probably caused by the bow shock sweeping across the wing.

Tunnel operational characteristics. - The minimum ejector pressures required for maintaining hypersonic flow at various combustor pressures is shown in figure 21 along with the standard tunnel operational boundaries discussed earlier. Results were obtained for combustor total pressures of 580, 1160, 1740, and 2180 psia using air (T_{tc} = 500 R) and combustion products (T_{tc} = 3060 R) for α = -4.5 and 10.5°. As with the CSTA model, the minimum operational boundary is between the standard boundaries and, hence, the model may be considered a small to medium blockage model.

CONCLUDING REMARKS

A 1/12th scale model of the Curved Surface Test Apparatus (CSTA), which will be used to study aerothermal loads and evaluate Thermal Protection Systems (TPS) on a fuselage-type configuration in the Langley 8-Foot High Temperature Structures Tunnel (8' HTST), was tested in the Langley 7-Inch Mach 7 Pilot Tunnel. The purpose of the pilot tunnel tests was to study the overall flow characteristics and define an envelope for testing the CSTA in the 8' HTST. This envelope is defined by the model angle of attack and tunnel operating pressures at which the flow field around the model remains realistic. Tests were then conducted using the scaled CSTA model with various wing configurations to select a wing geometry with the most favorable characteristics for conducting TPS evaluation for curved and intersecting surfaces. The test envelope of the selected wing configuration, which is beveled 30° on the leading edge, was also obtained.

Results indicate that the CSTA can be tested with no shock interference at angles of attack up to 15.5 degrees for combustor pressures above 580

15

psia. For the same pressure range, the wing configuration can be tested at angles of attack up to 10.5 degrees. In both cases the angle of attack is limited to 5.5 degrees at a pressure of 580 psia because of shock interference with the model flow field. The base pressure for the CSTA model and wing configuration was at the expected low level for most test conditions. However, a high base pressure was obtained at certain test conditions in which ambient temperature air was used as the test medium. Improved performance was demonstrated for high temperature conditions, using combustion products as the test medium, but the possibility of a high base pressure should be evaluated during the initial flow studies in the 8' HTST. The tunnel operational performance for both the CSTA model and wing configuration was representative of the performance for a small to medium blockage model for the range of angles of attack tested. Results generally indicate that the CSTA and wing configuration will provide a useful test bed for aerothermal loads and thermal structural concept evaluation over a broad range of flow conditions in the 8' HTST.

NASA
L-80-6916

(a) Three-quarter front view.
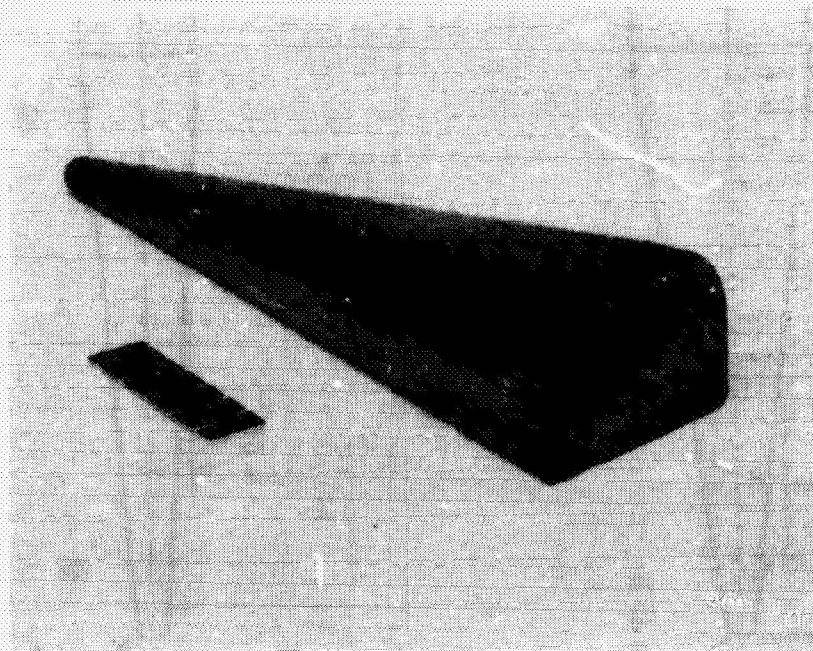
NASA
L-80-6917

(b) Three-quarter rear view.

Figure 1. - Photographs of the CSTA model.

3.02

9.70

7.59°

0.25 R

Top view

Isometric view

2.00

4.50°

α

Side view

1.00 R

0.33 R

Tangent line
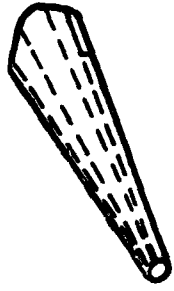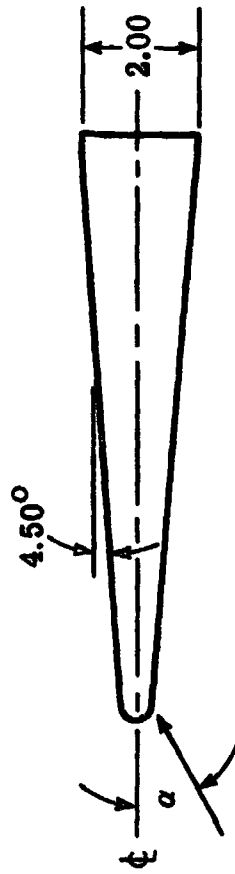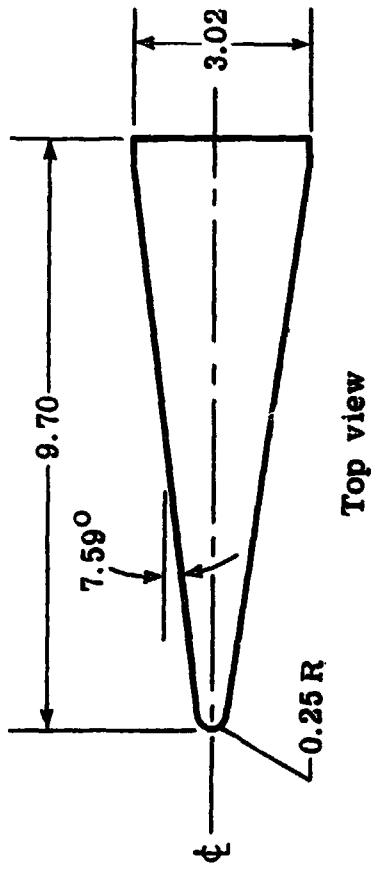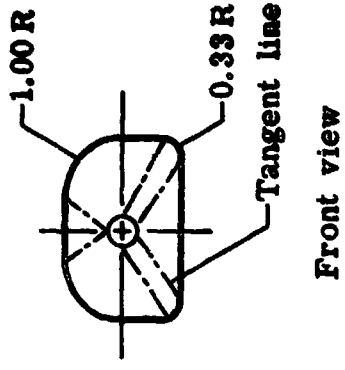
Front view

Figure 2. - Sketch of the CSTA model. All dimensions are in inches.

0.66

Rear view

3.5°

Wing

Body

Isometric view

7.00

2.25

4.92

1.92

45°

Top view

A

A

Side view

0.66

0.33 R
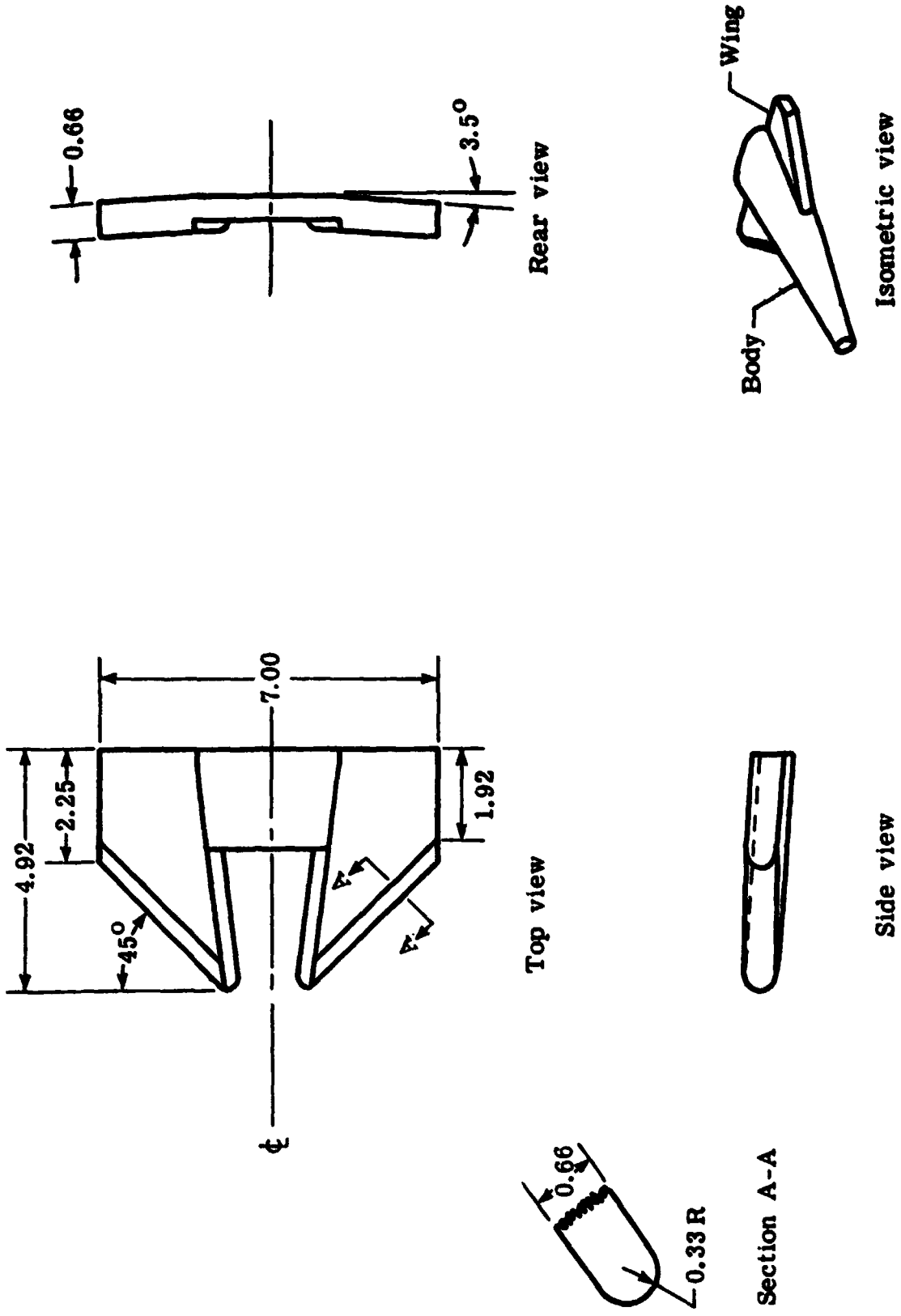
Section A-A

(a) Configuration I.

Figure 3. - Sketch of wings for various wing configurations. All dimensions are in inches.

0.66

Rear view

3.5°

0.66

0.33R

Section A-A

6.00

4.32

2.00

45°

1.67
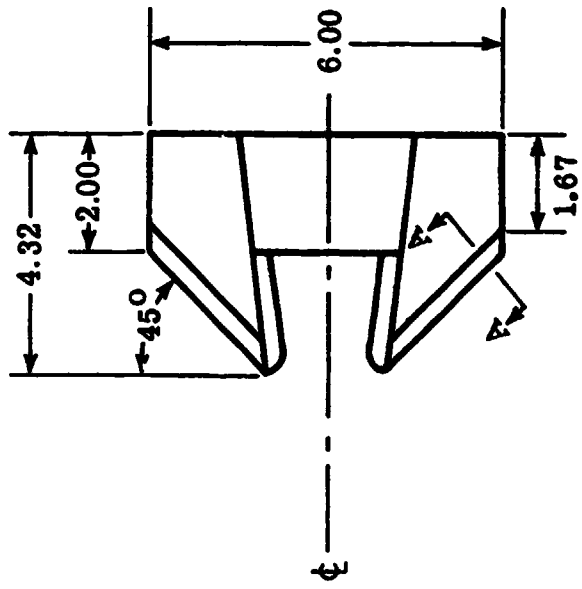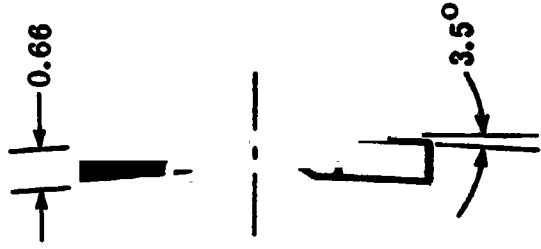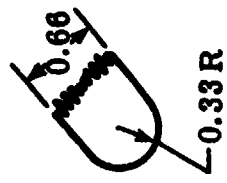
Top view

Side view

(b) Configuration II.

Figure 3. - Continued.

0.66

Rear view

3.5°

0.66

0.33 R

Section A–A

5.00

2.94

1.55

1.22

45°

A

A

Top view

∉
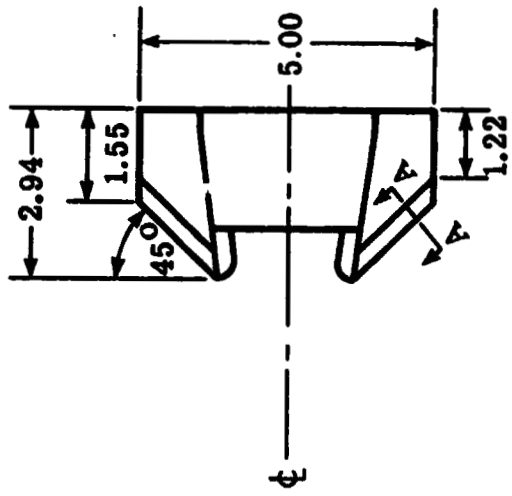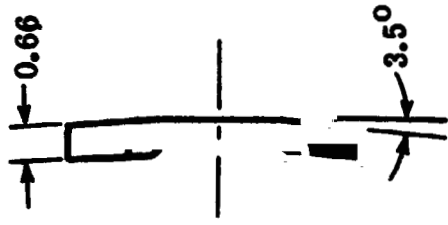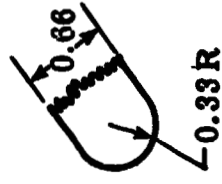
Side view

(c) Configuration III.

Figure 3. – Continued.

0.33

3.5°

Rear view

0.33

0.17R

Section A-A

6.00

4.32

2.00

1.83

45°
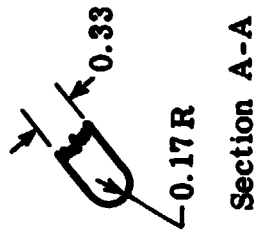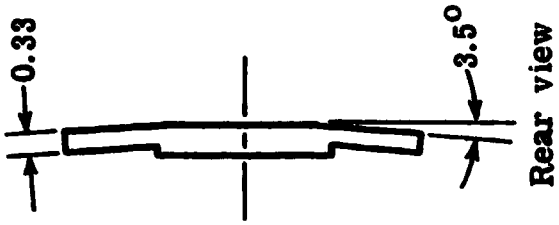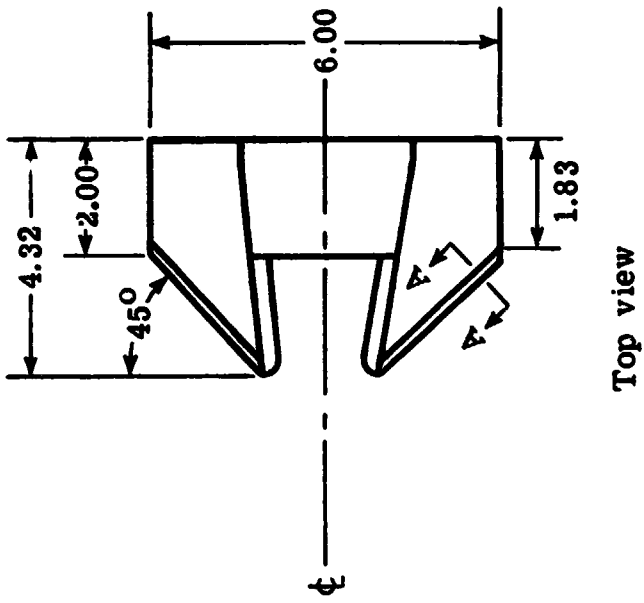
Top view

Side view

(d) Configuration IV.

Figure 3. – Continued.

0.66

Rear view

3.5°

0.66

1.75 R

.860

0.17 R

Section A-A

6.00

4.92

2.25

45°

1.67

A

A
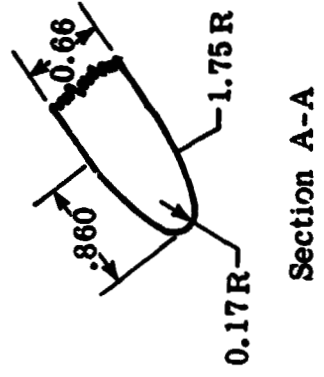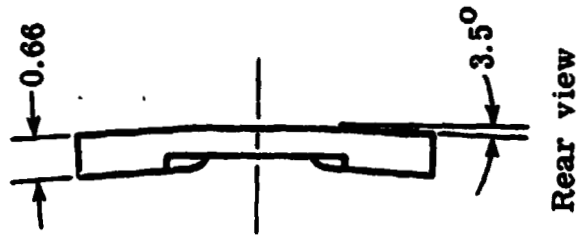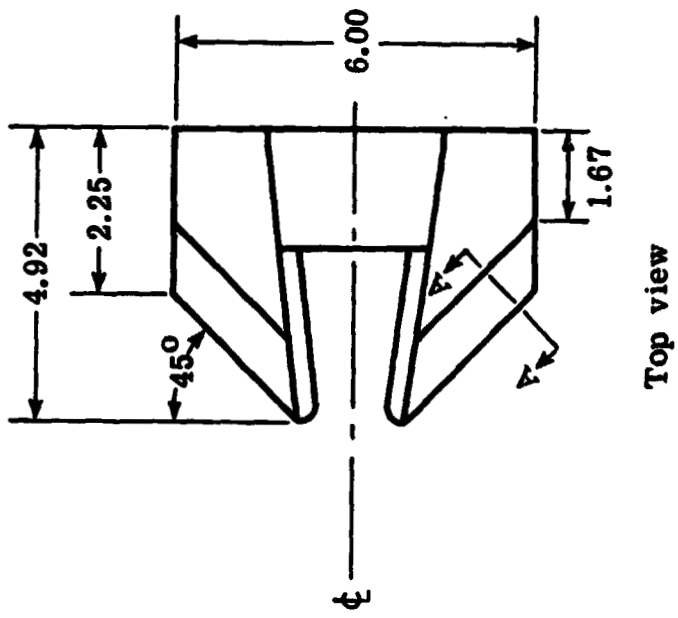
Top view

Side view

(e) Configuration V.

Figure 3. - Continued.

0.66

Rear view

3.5°

0.66

21°

Section A-A

6.00

2.25

4.92

1.67

45°
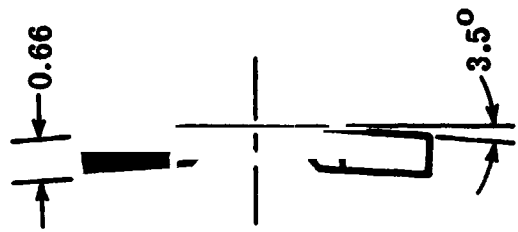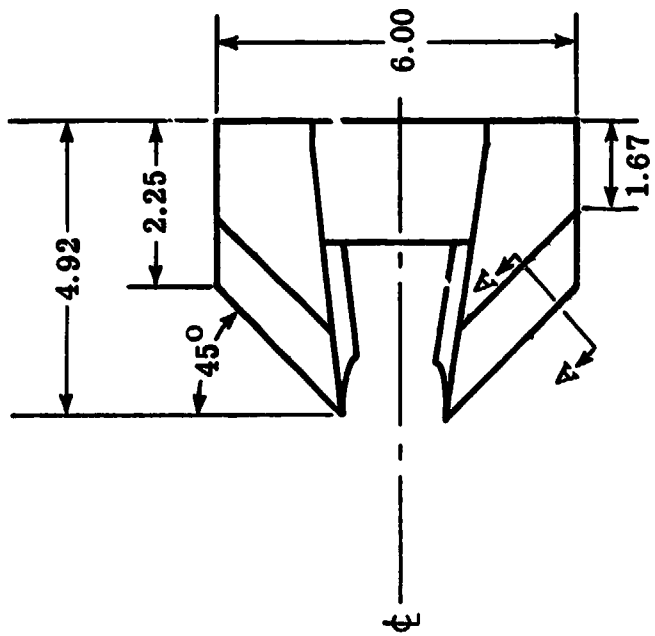
Top view
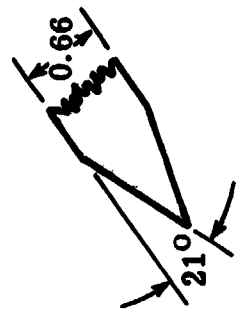
Side view

(f) Configuration VI.

Figure 3. - Continued.

0.50

Rear view

0.50

0.015 R

30°

Section A-A

6.00

2.25

4.92

1.67

45°

A

A

Top view

Side view
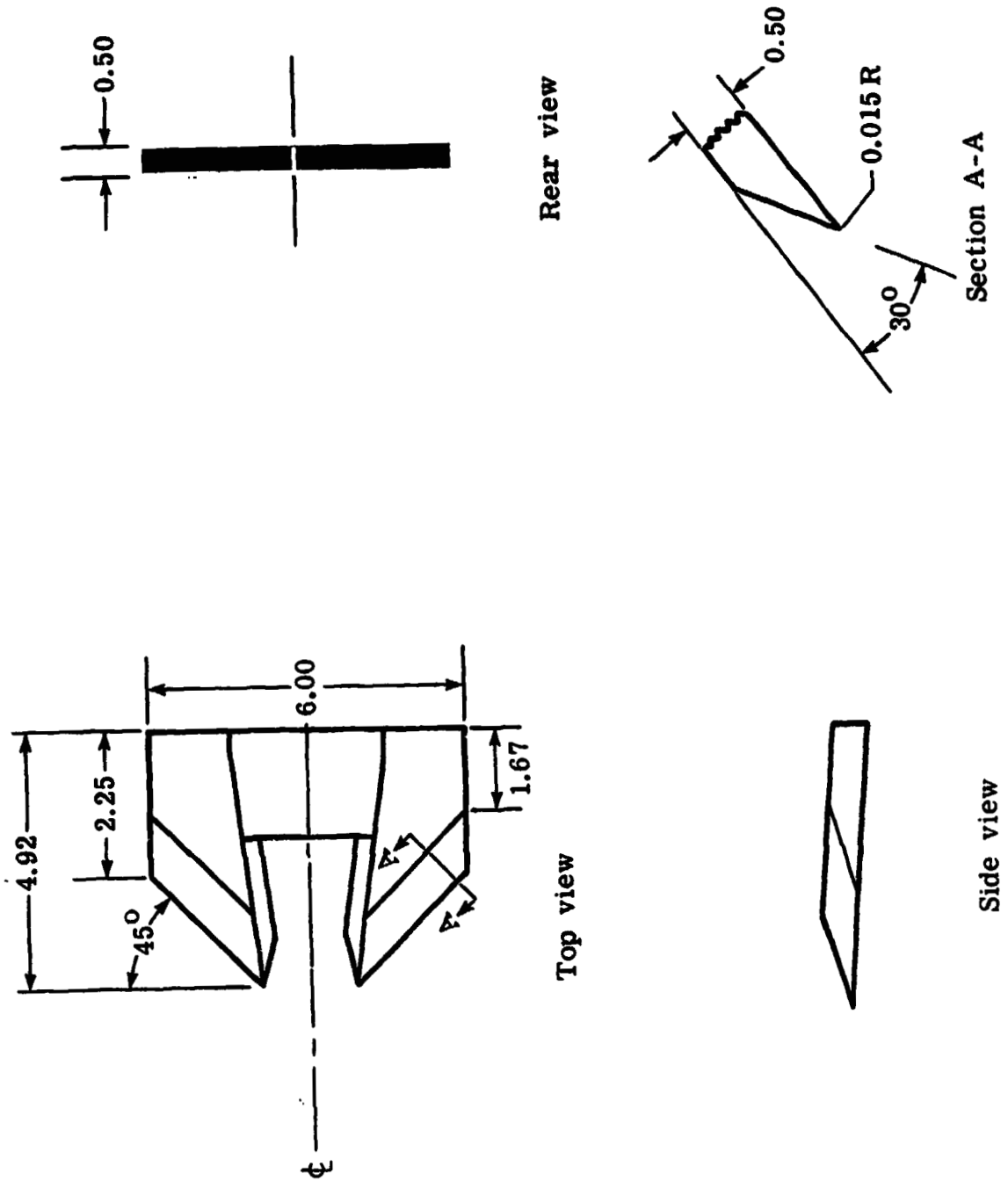
(g) Configuration VII.

Figure 3. - Concluded.

Fairing
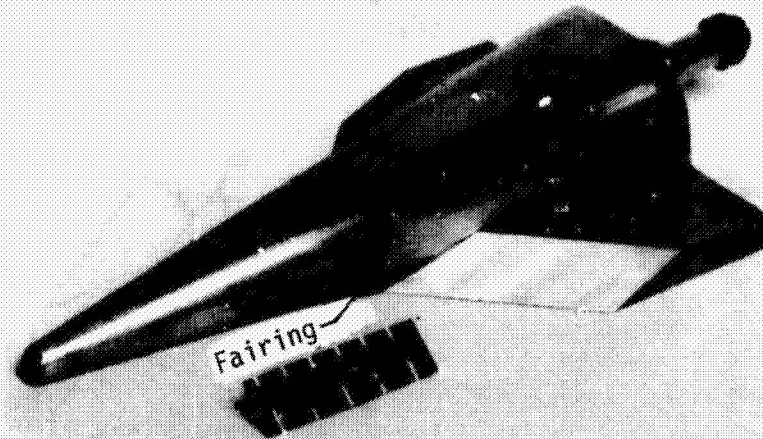
NASA
L-80-10,556

(a) Three-quarter front view.
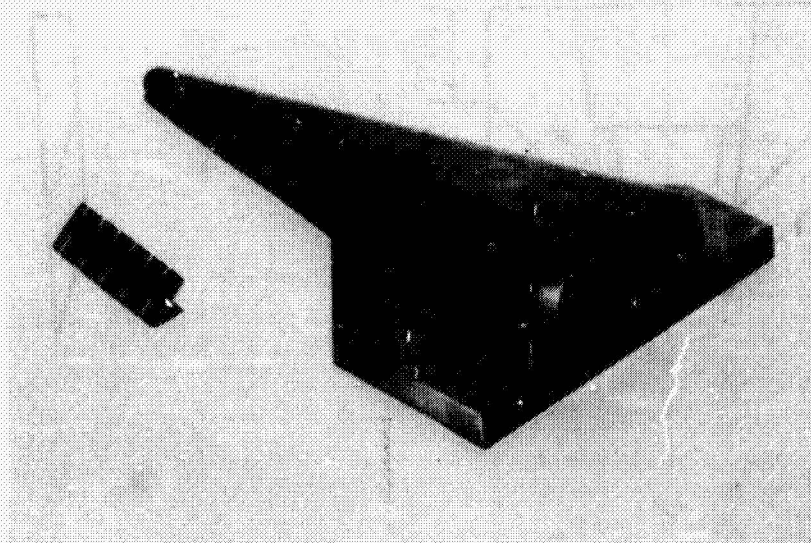
NASA
L-81-6301

(b) Three-quarter rear view.

Figure 4. - Photographs of Configuration VII.
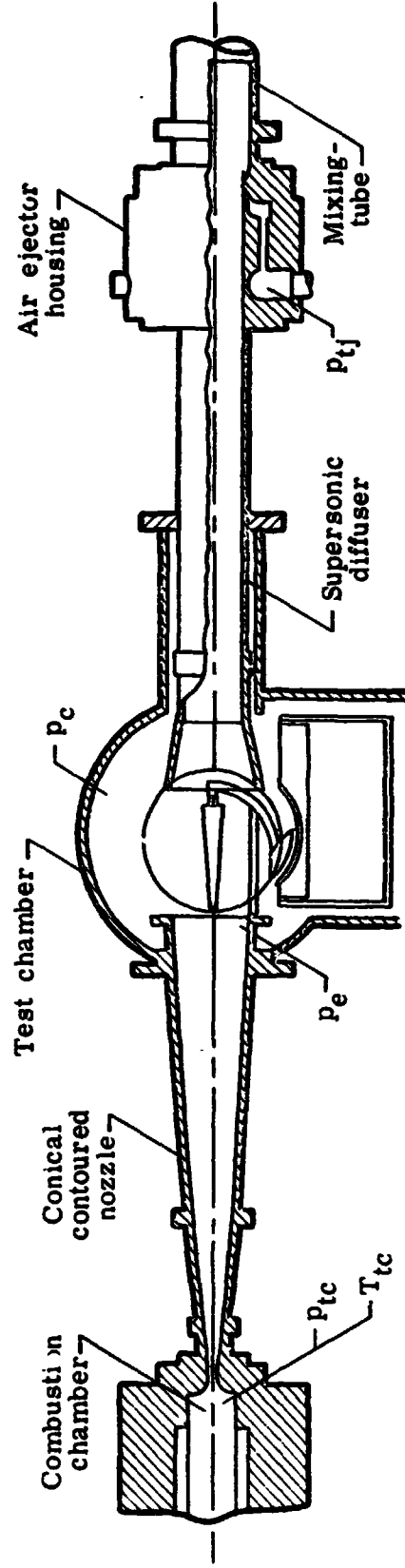
Figure 5. - Schematic of 7 inch Mach 7 pilot tunnel at Langley Research Center.
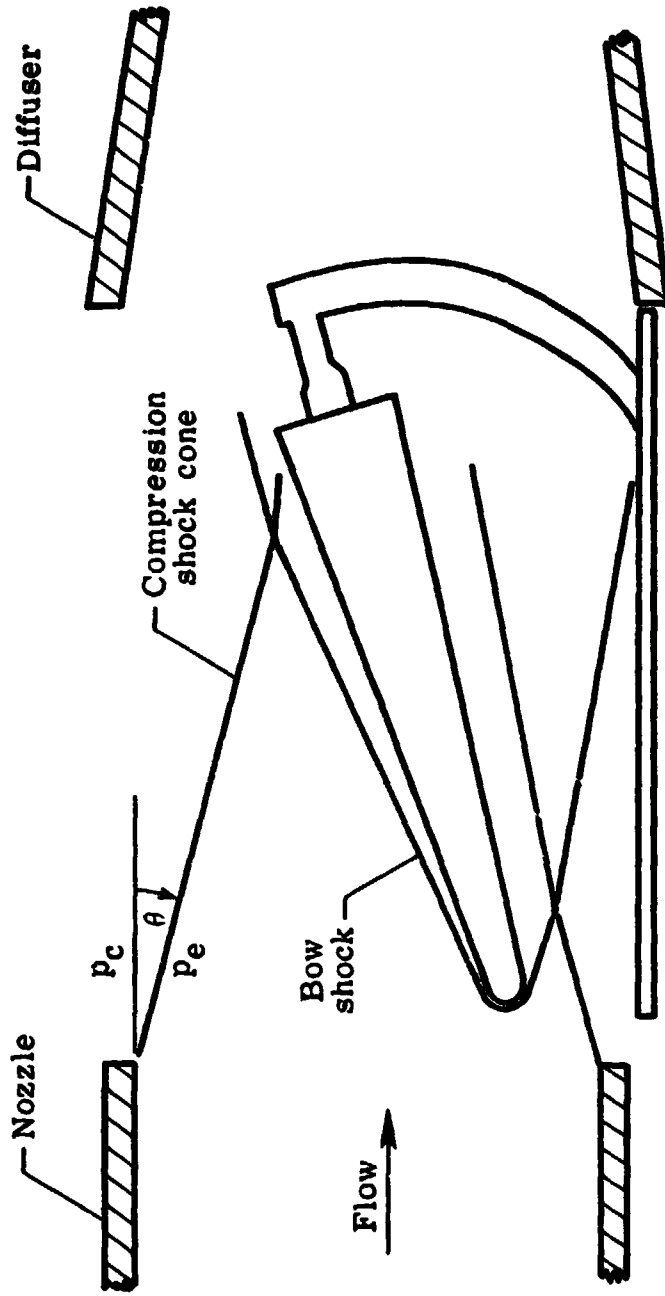
Figure 6. - Compression shock cone formation at the nozzle exit due to flow blockage.
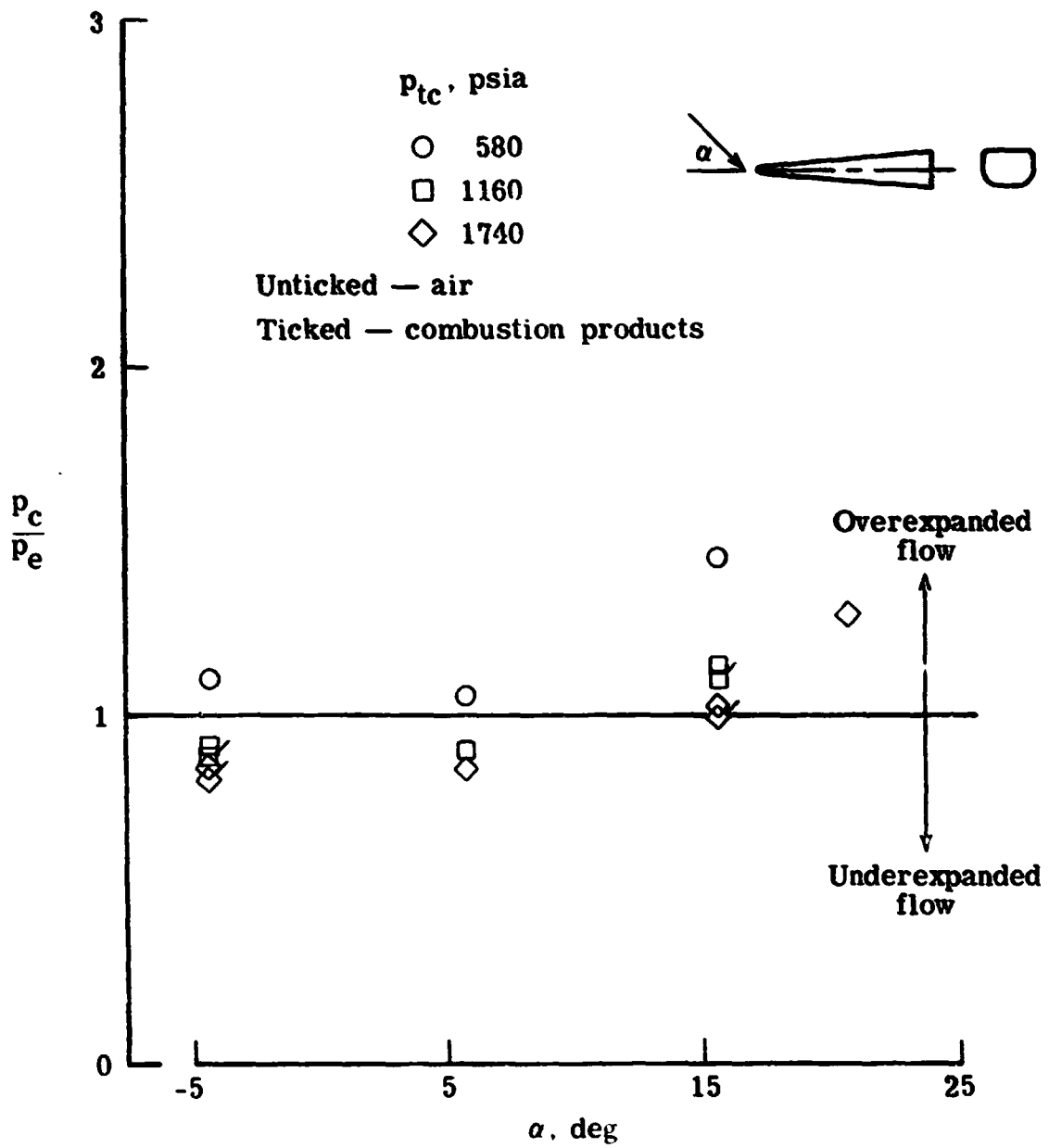
Figure 7. - Test chamber to nozzle exit pressure ratios for the CSTA model at various test conditions.
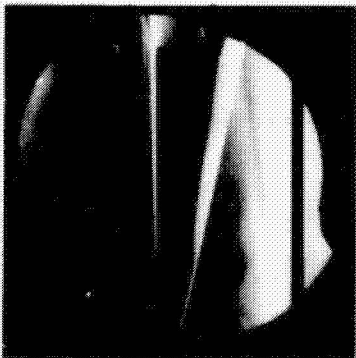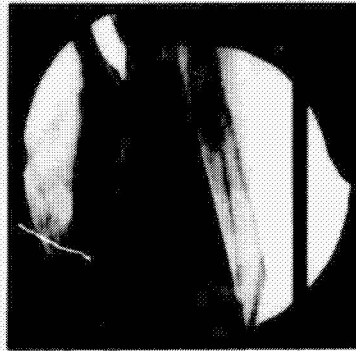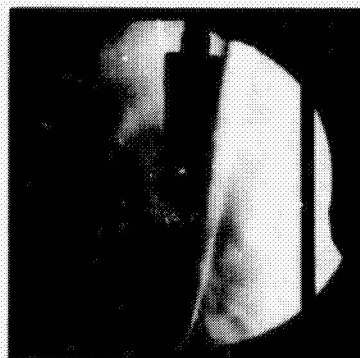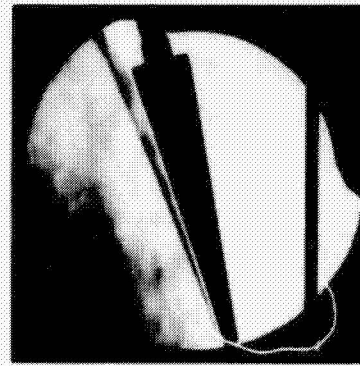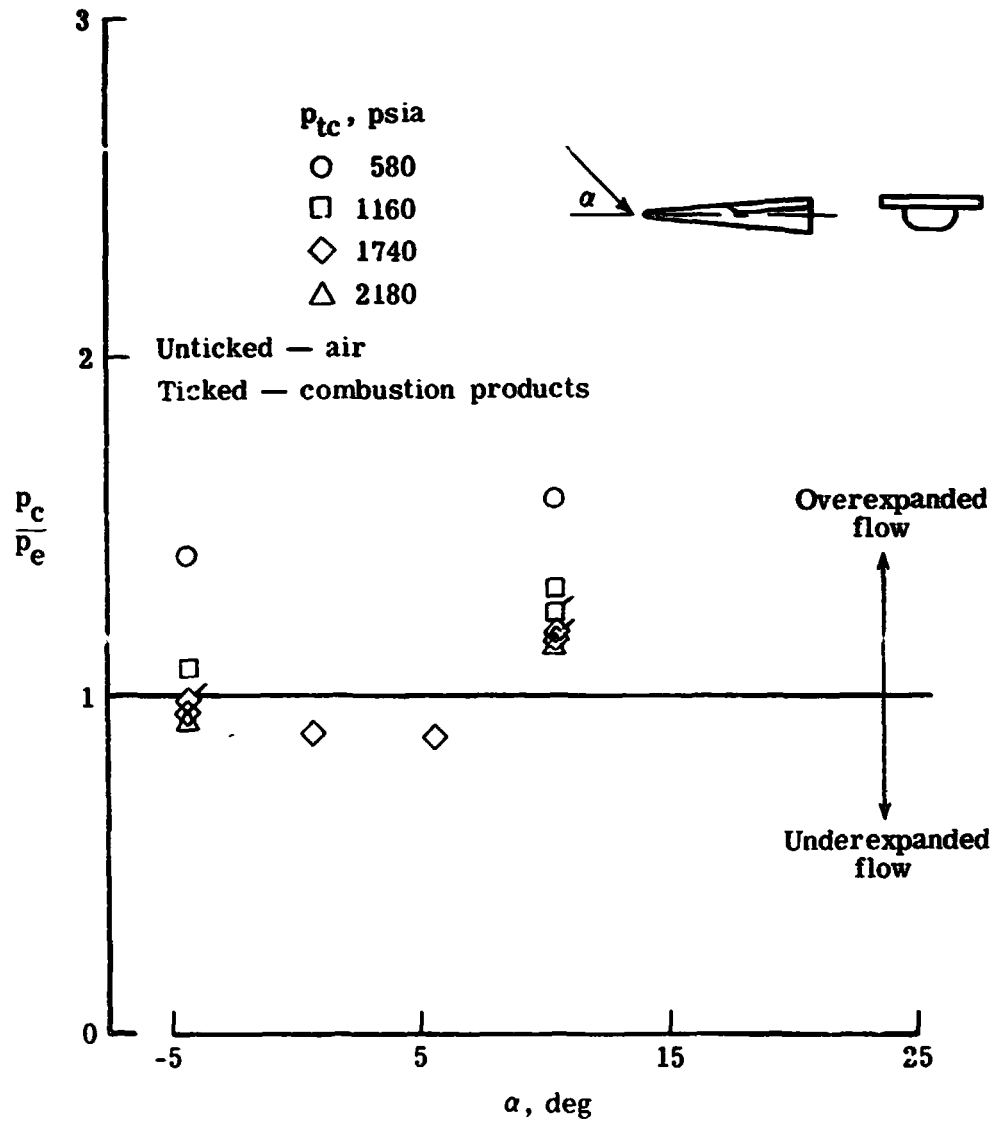
Figure 8. – Schlieren photographs of the CSTA model at various angles of attack, pt_c = 1740 psia.

$p_{tc} = 1740$ psia

$p_{tc} = 1160$ psia

$p_{tc} = 580$ psia

Air
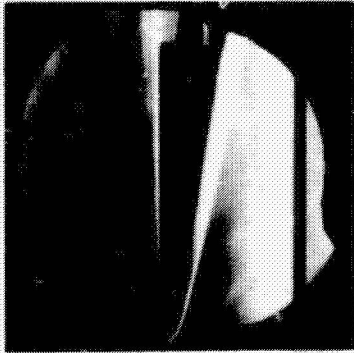
$p_{tc} = 1740$ psia

$p_{tc} = 1160$ psia

Combustion products

(a) $\alpha = -4.5°$

Figure 9. - Schlieren photographs of the CSTA model for various combustor total pressures.
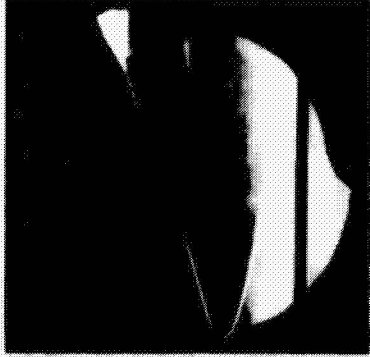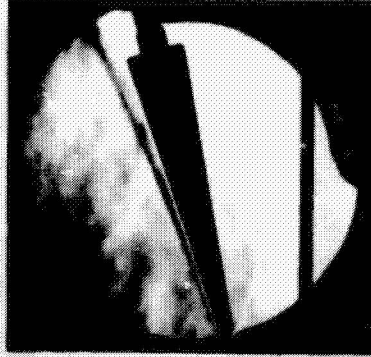
p_{tc} = 1740 psia

p_{tc} = 1740 psia
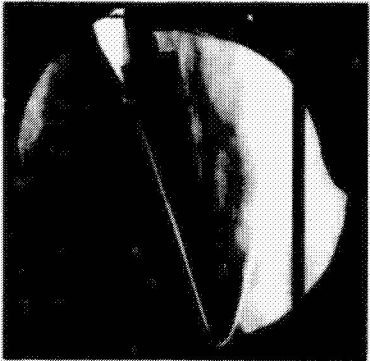
p_{tc} = 1160 psia

Air

p_{tc} = 1160 psia

Combustion products

p_{tc} = 580 psia

(b) α = 15.5°

Figure 9. - Concluded.

Trailing recompression shock

Wake shear layer

Bow shock

Flow

Nozzle

Mach disk

Slip streamline
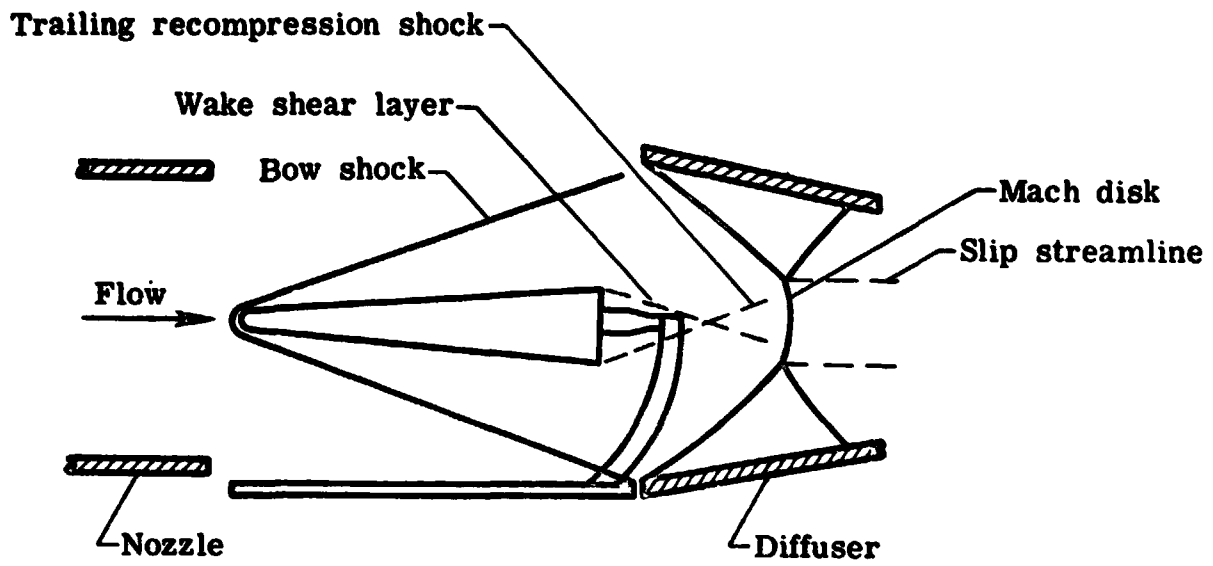
Diffuser

(a) Wake convergence resulting in a low base pressure.

Wake shear layer

Bow shock

Flow

Nozzle

Mach disk

Slip streamline
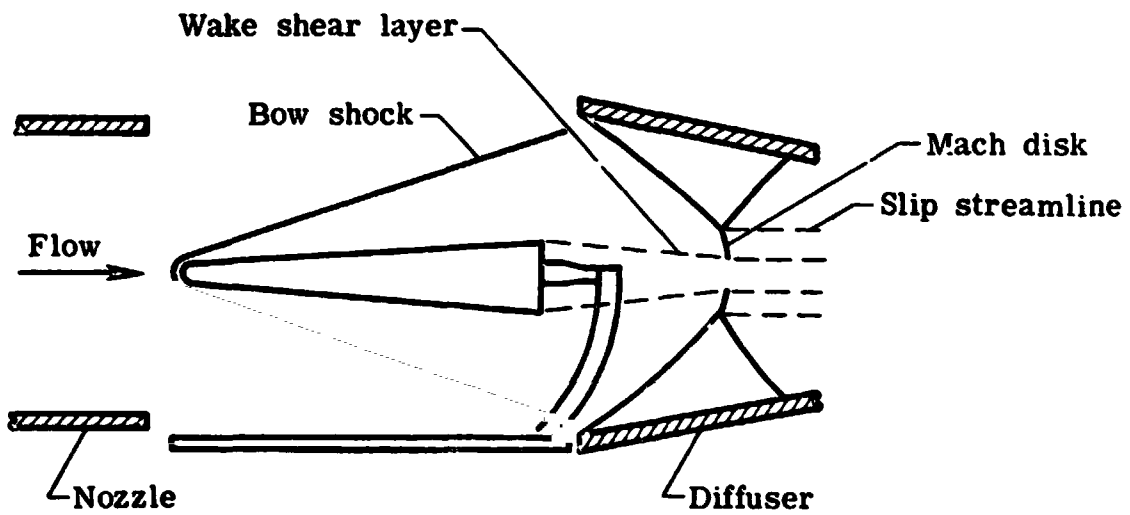
Diffuser

(b) Wake intersection with a Mach disk resulting in a high base pressure.

Figure 10. - Illustration of possible wake-shock interaction in the diffuser.
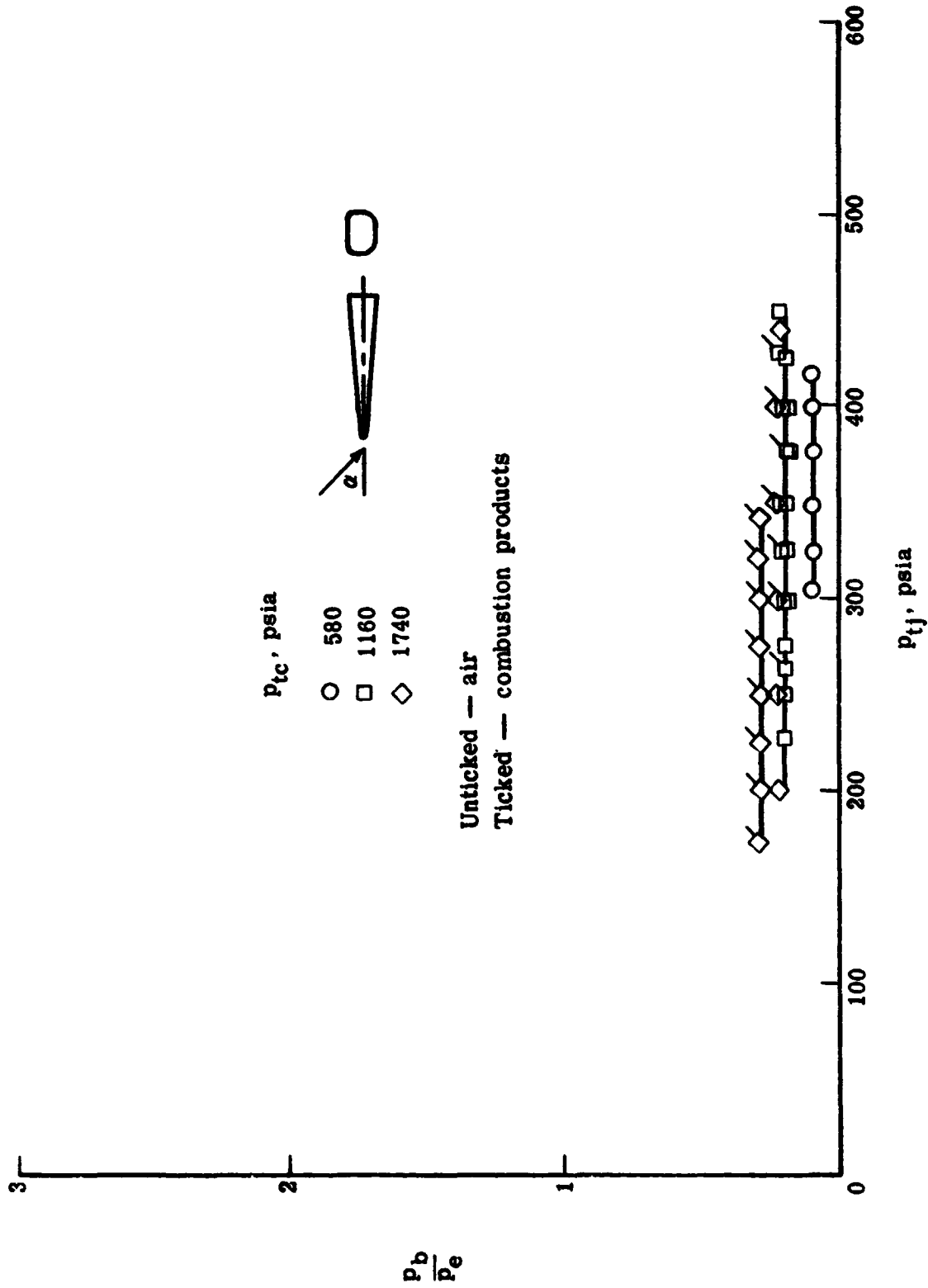
Figure 11. - Base pressure to nozzle exit pressure ratios for the CSTA model at various test conditions.

(a) α = -4.5°

P_{tc}, psia

○ 580
□ 1160
◇ 1740

Unticked — air
Ticked — combustion products

$\dfrac{p_b}{p_e}$

P_{tj}, psia
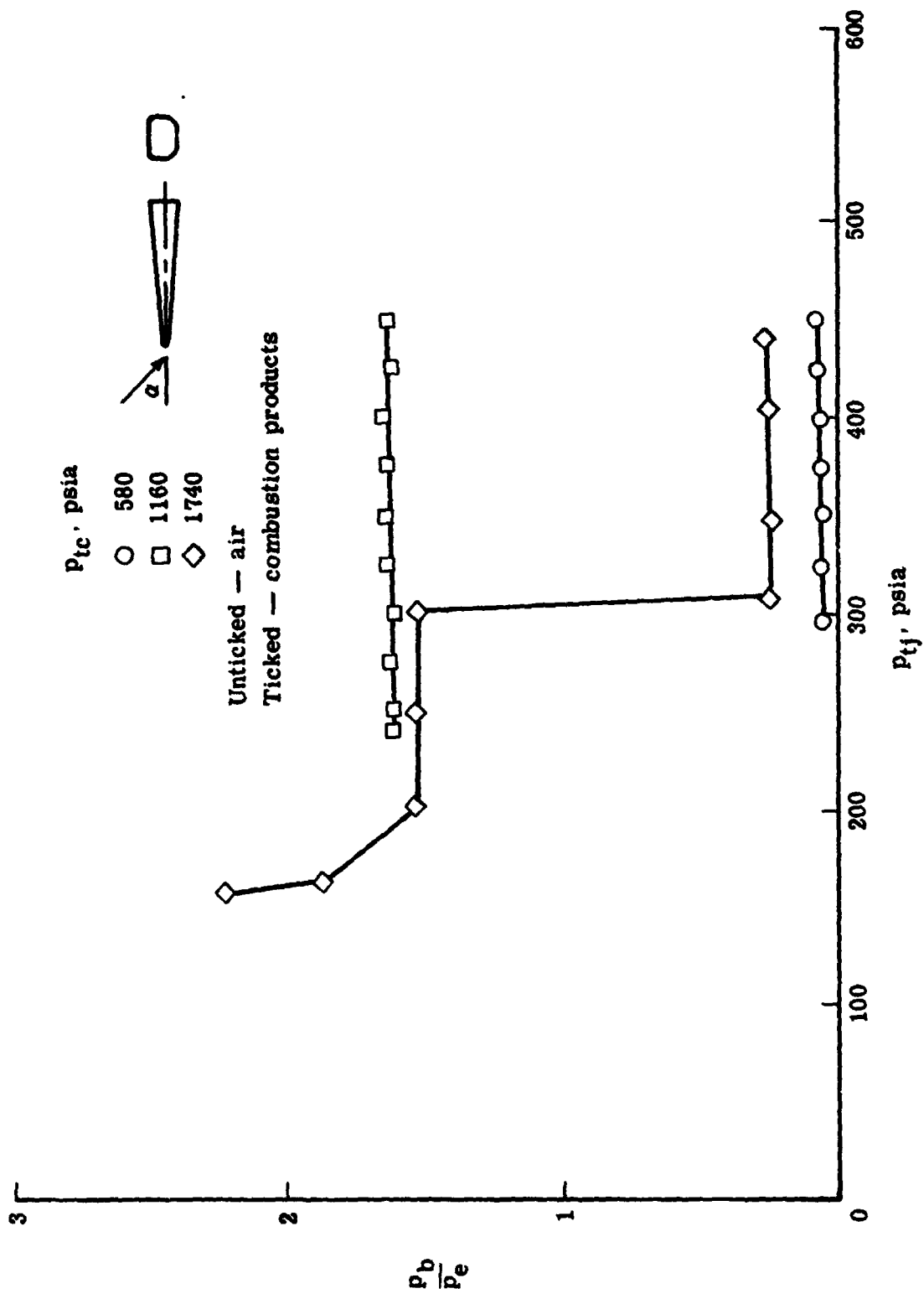
(b) $\alpha = 5.5°$

Figure 11. - Continued.

P_{tc}, psia

○ 580
□ 1160
◇ 1740

Unticked — air
Ticked — combustion products

(c) α = 15.5°
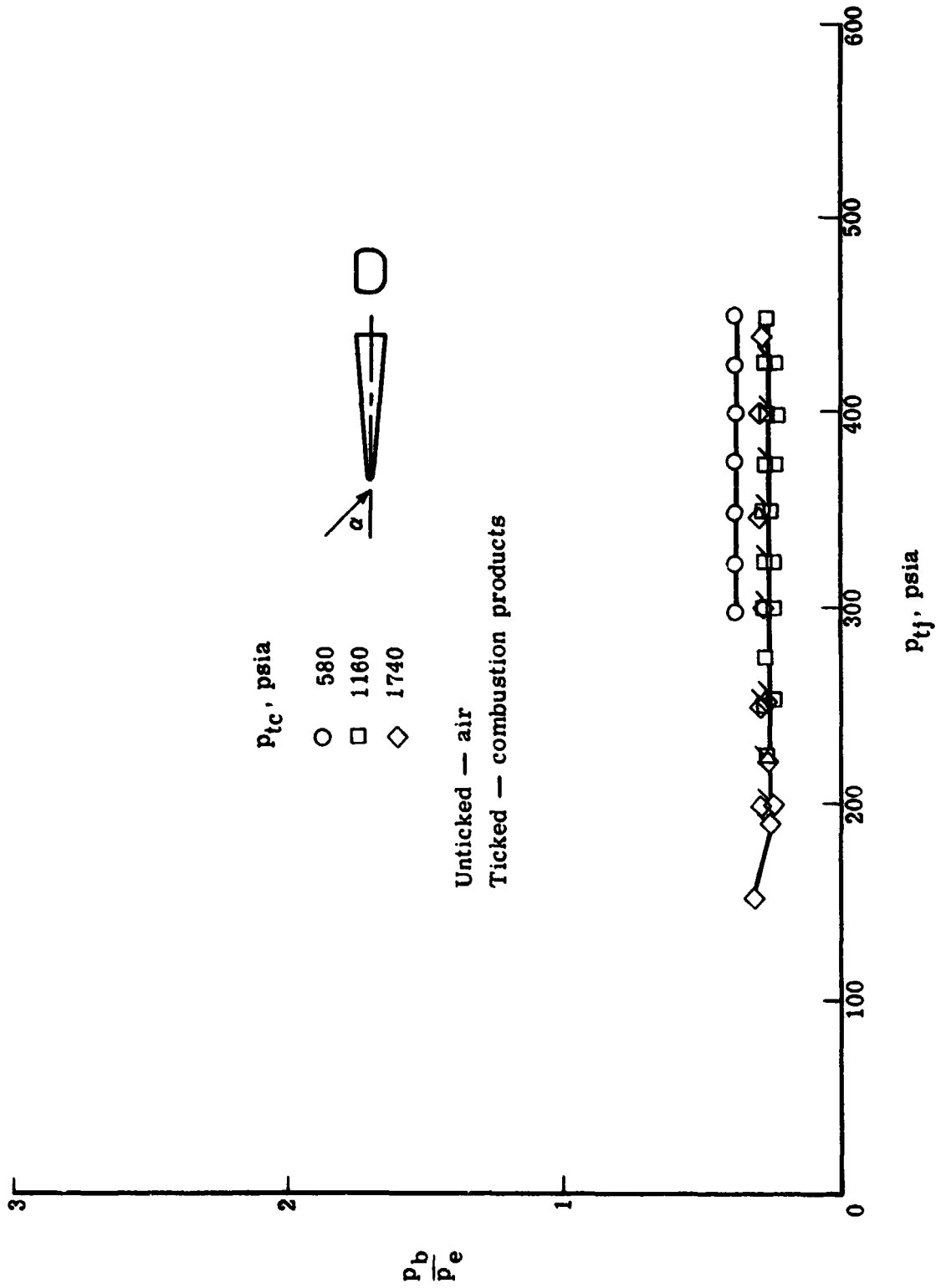
Figure 11. – Concluded.
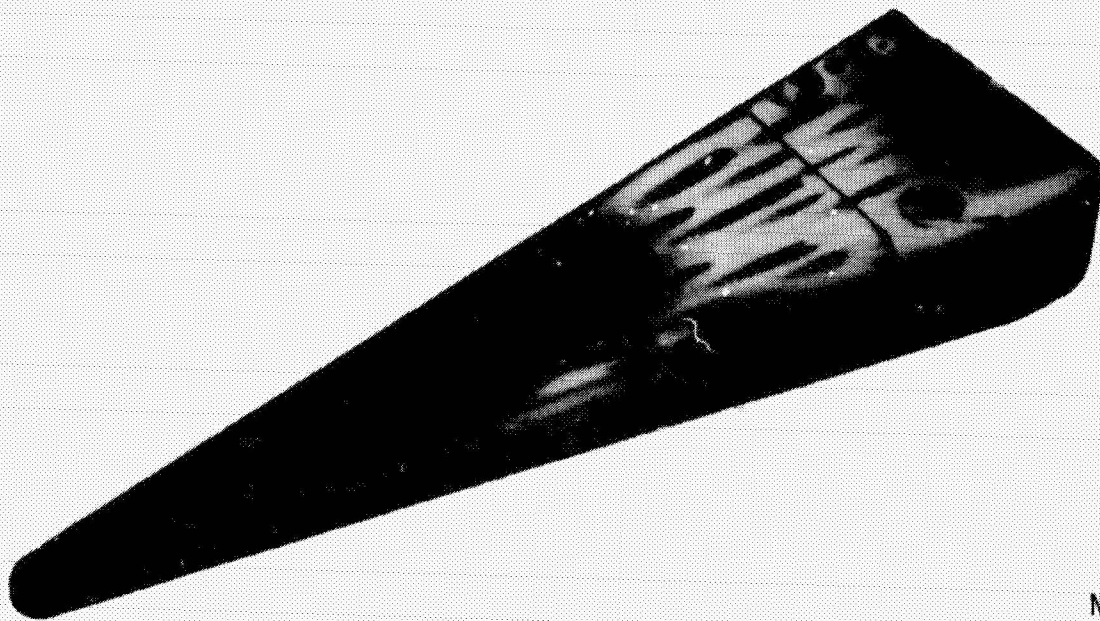
NASA
L-81-3587

(a) Windward flat and chine surfaces.

NASA
L-81-3367

(b) Leeward flat and chine surfaces.

Figure 12. - Oil-flow pattern for the CSTA model in air, α = 15.5°, p_{tc} = 1740 psia
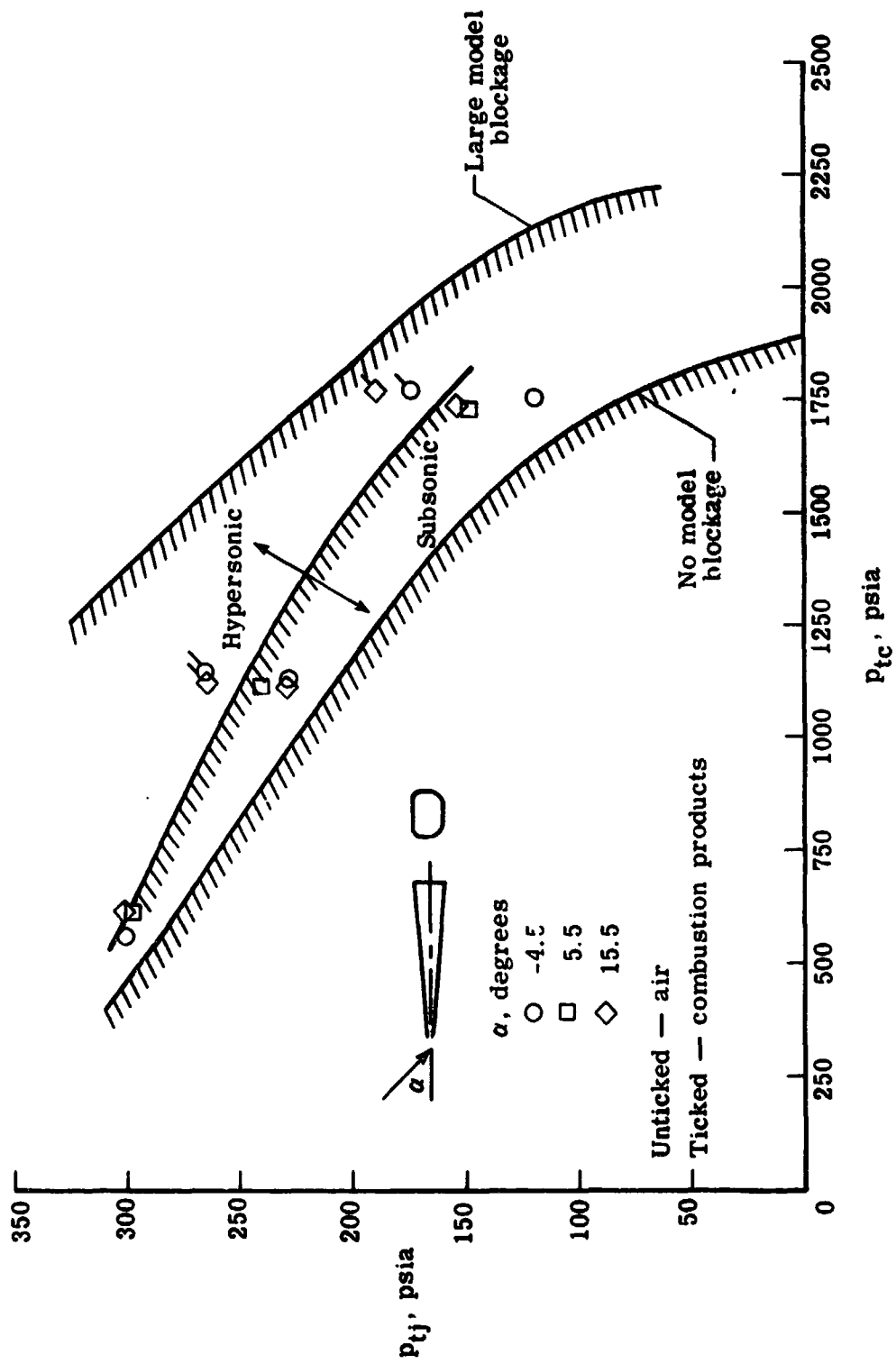
Figure 13. - Tunnel operational characteristics for the CSTA model.
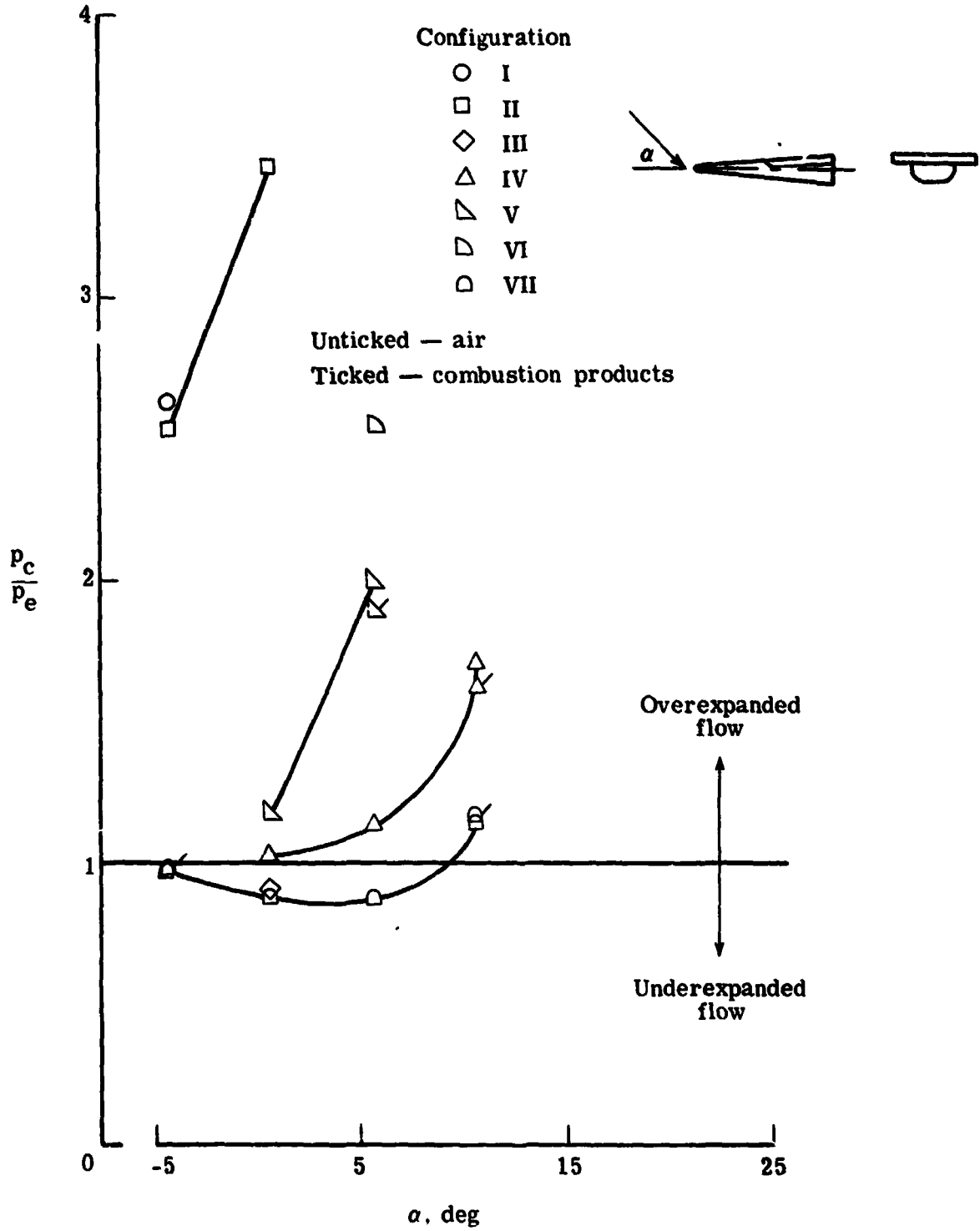
Figure 14. - Test chamber to nozzle exit pressure ratios for configurations I through VII, p_{tc} = 1740 psia.

$\alpha = -4.5^{\circ}$

Configuration I

$\alpha = -4.5^{\circ}$ $\alpha = 0.5^{\circ}$

Configuration II

$\alpha = 0.5^{\circ}$

Configuration III

(a) Effect of planform area on flow blockage
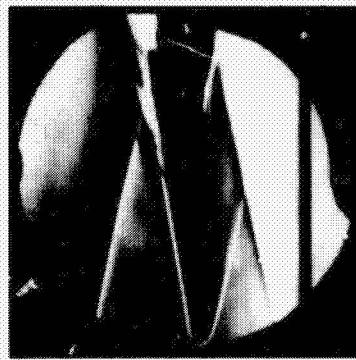
Configuration IV

Configuration V   Configuration VI

Configuration VII
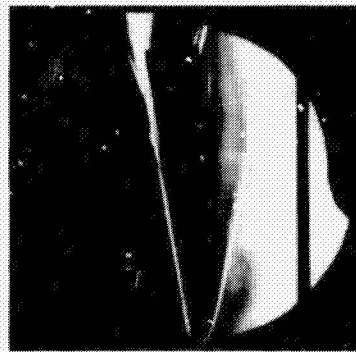
(b) Effect of leading edge on flow blockage, $\alpha = 5.5^{\circ}$

Figure 15. - Schlieren photographs of configurations I through VII in air,
Ptc = 1740 psia.

Figure 16. - Test chamber to nozzle exit pressure ratios for configuration VII at various test conditions.

$\alpha = -4.5^o$ $\alpha = 0.5^o$ $\alpha = 5.5^o$ $\alpha = 10.5^o$

Air

$\alpha = -4.5^o$ $\alpha = 10.5^o$
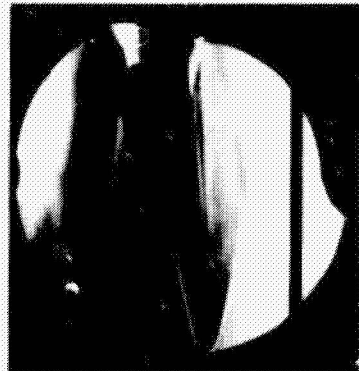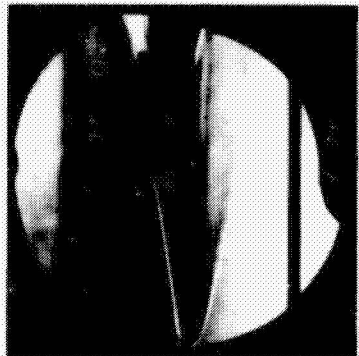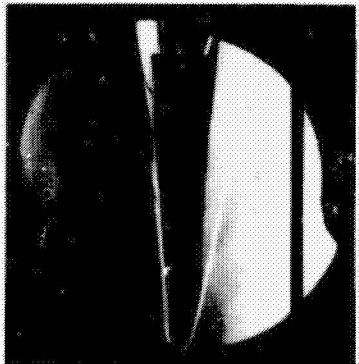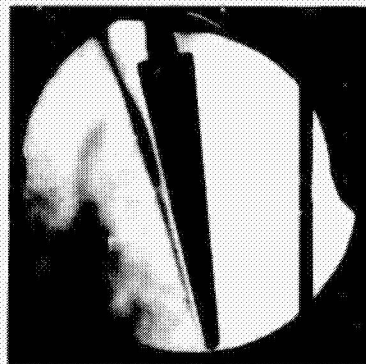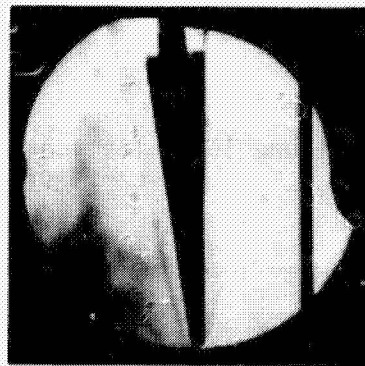
Conbustion products

Figure 17. - Schlieren photographs of configuration VII for various angles of attack. P_{tc} = 1740 psia.
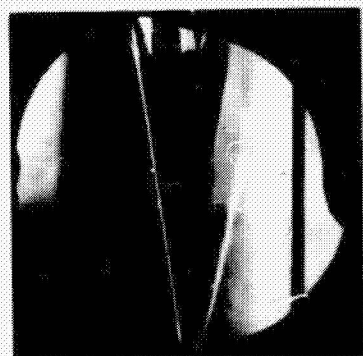
p_{tc} = 2180 psia

p_{tc} = 1740 psia

Air

p_{tc} = 580 psia
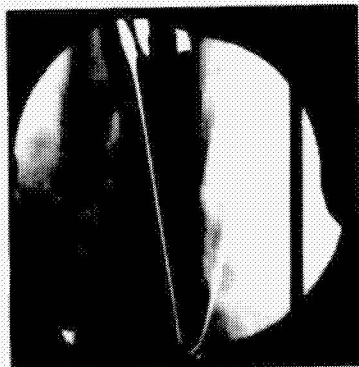
p_{tc} = 1740 psia

Combustion products

(a) α = -4.5°

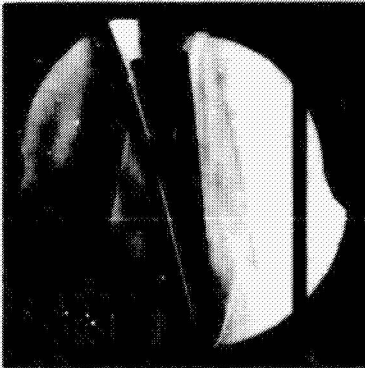Figure 18. - Schlieren photographs of configurations VII for various combustor total pressures.
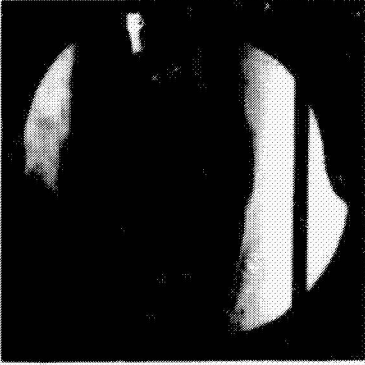
p_{tc} = 2180 psia

p_{tc} = 1740 psia

p_{tc} = 1160 psia

p_{tc} = 580 psia

Air

p_{tc} = 1740 psia

p_{tc} = 1160 psia

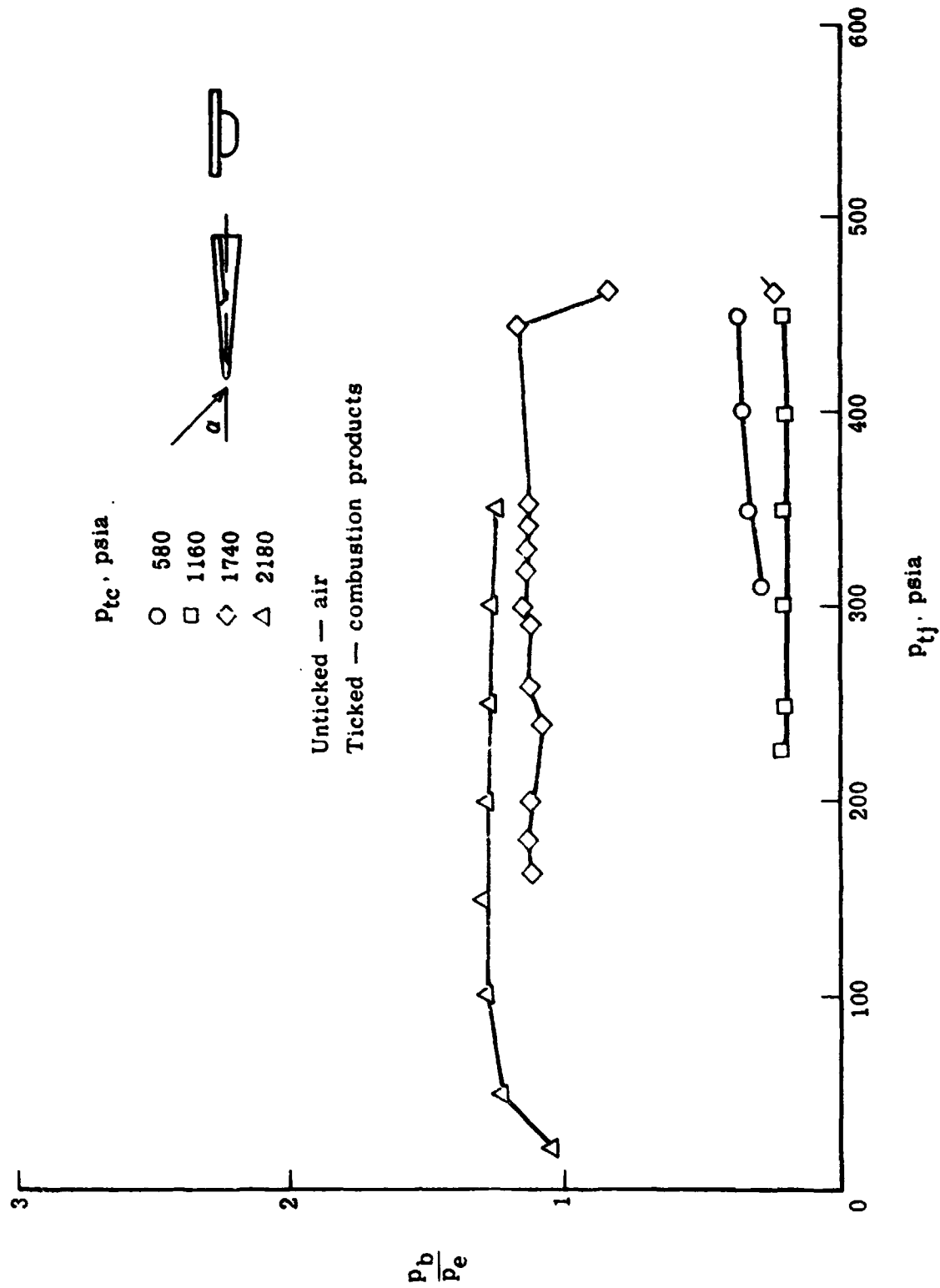Combustion products

(b) α = 10.5°

Figure 18. - Concluded.

P_{tc}, psia

○ 580
□ 1160
◇ 1740
△ 2180

Unticked — air
Ticked — combustion products

$\frac{P_b}{P_e}$

P_{tj}, psia

(a) $\alpha = -4.5°$
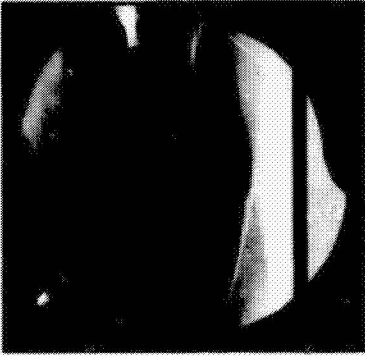
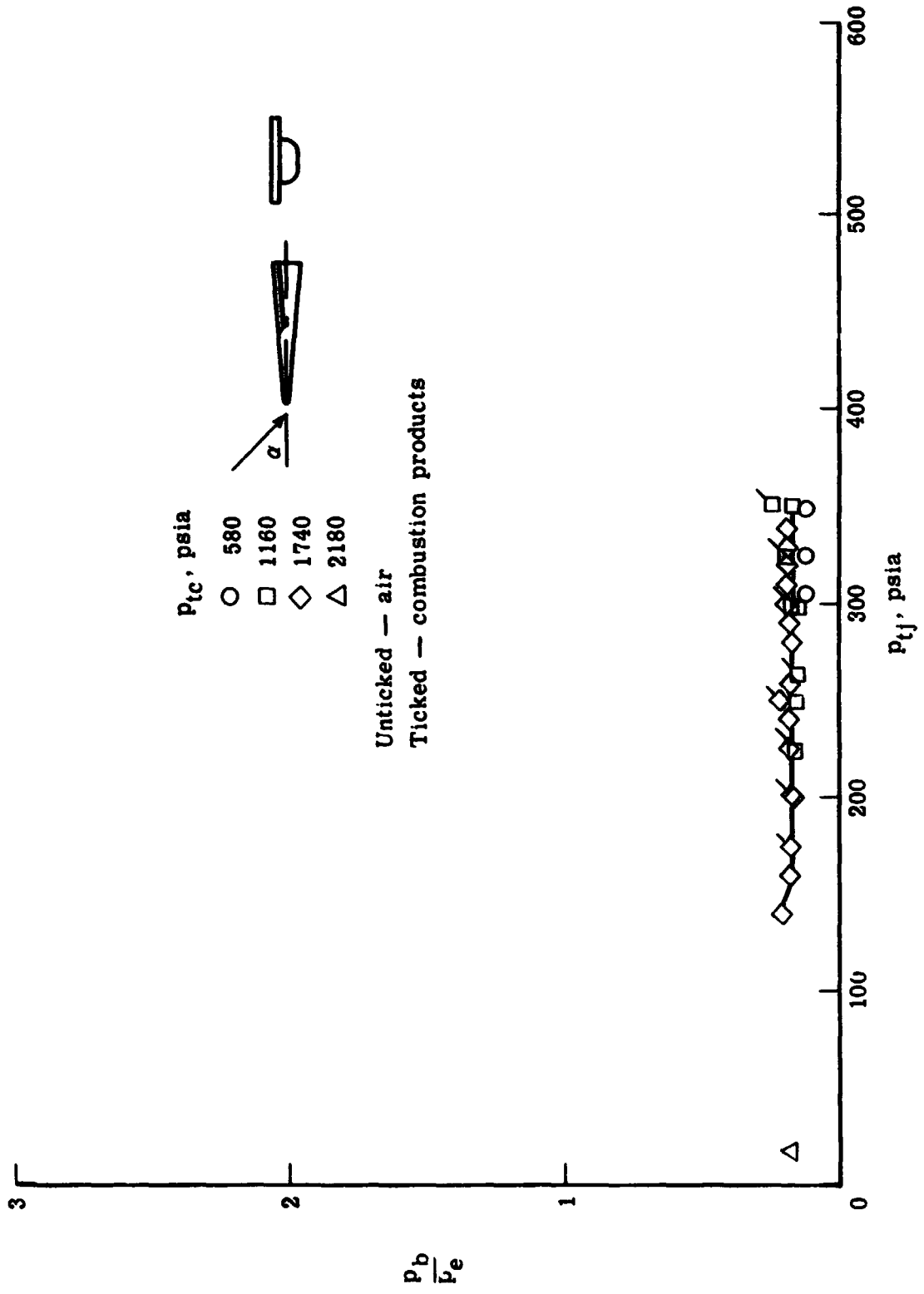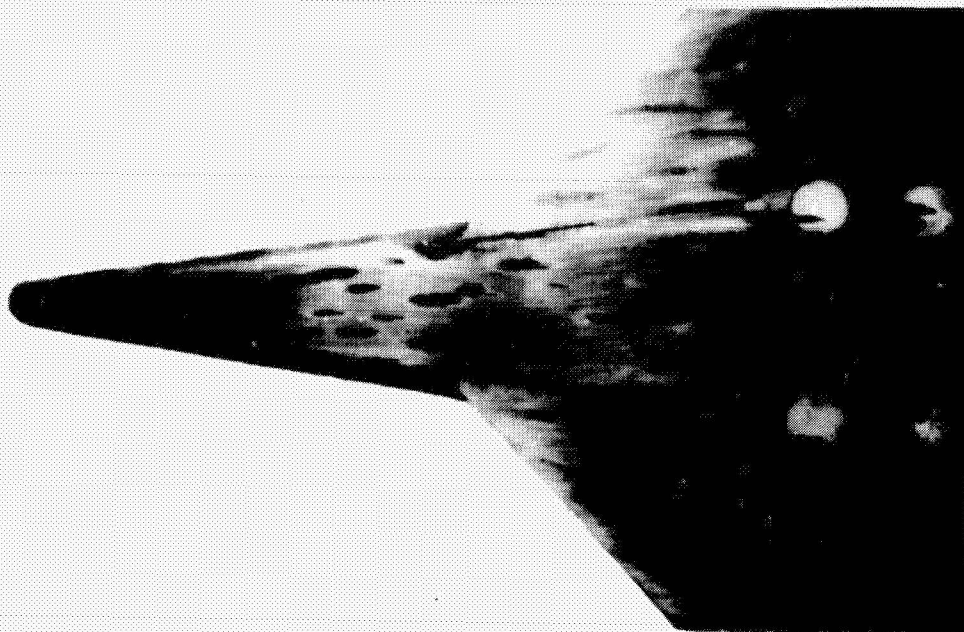Figure 19. – Base pressure to nozzle exit pressure ratios for configuration VII at various test conditions.

(b) α = 10.5°

Figure 19. - Concluded.

NASA
L-81-2318

(a) Windward flat surface.

NASA
L-81-2317

(b) Leeward flat and chine surfaces.

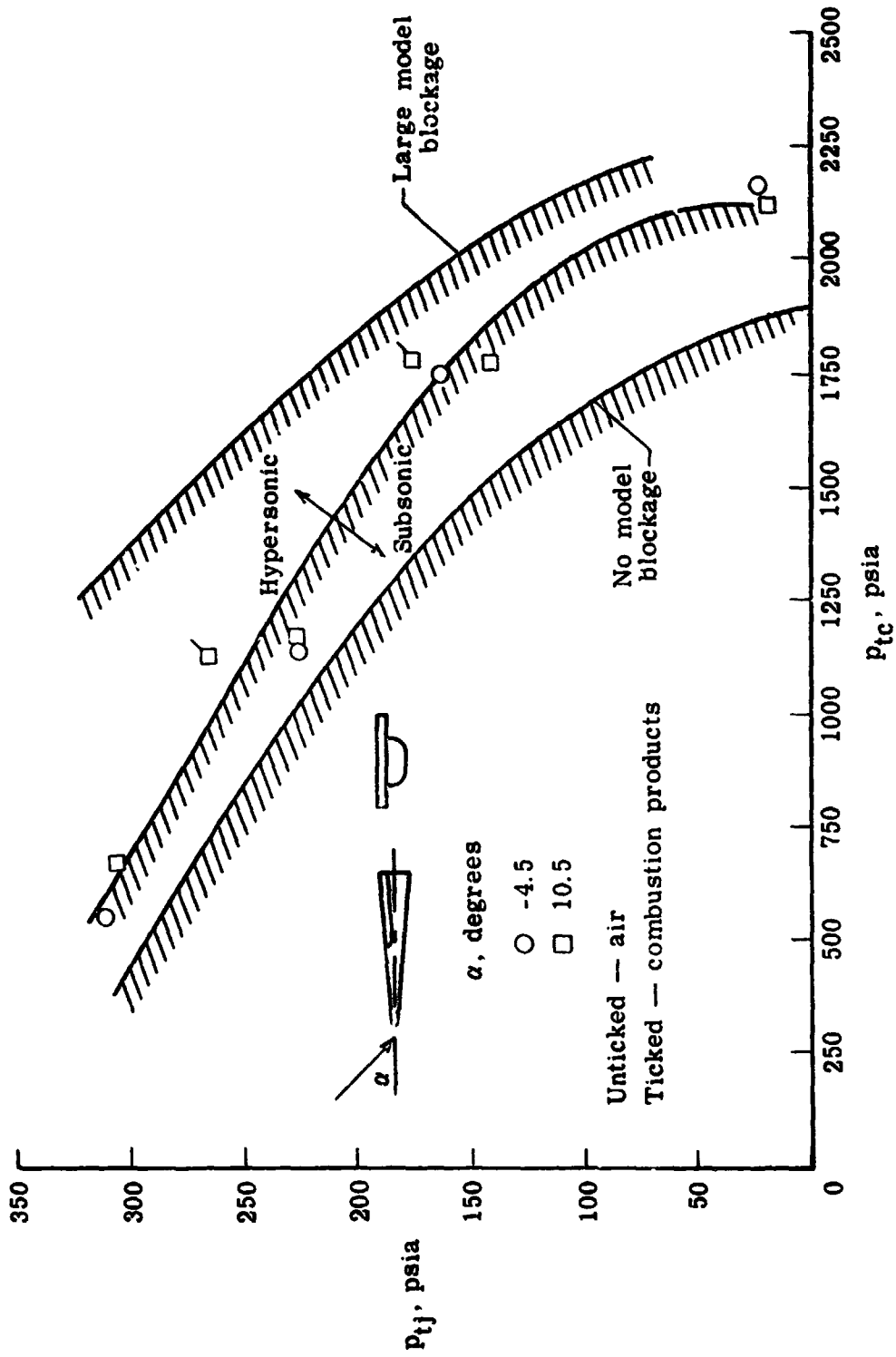Figure 20. - Oil-flow pattern for configuration VII in air, $\alpha = 10.5°$, $P_{tc} = 1740$ psia.

Figure 21. - Tunnel operational characteristics for configuration VII.